PERGAMON

International Journal of Solids and Structures 37 (2000) 6795–6824

INTERNATIONAL JOURNAL OF SOLIDS and STRUCTURES

www.elsevier.com/locate/ijsolstr

Buckling and post-buckling analysis of stiffened panels in wing box structures

Eduard Riks

Faculty of Aerospace Engineering, Kluyverweg 1, Technical University of Delft, NL-2600 GB Delft, Netherlands

Received 10 November 1999

Abstract

The finite strip method has successfully been applied for the calculation of the buckling load of stiffened panels in wing box structures. This article describes an implementation of the finite strip method that extends the scope of the analysis of the determination of the post-buckling stiffness of these panels. © 2000 Published by Elsevier Science Ltd.

Keywords: Buckling and post-buckling analysis; Stiffened panels; Box structures

1. Introduction

1.1. The panel problem

Wing box structures usually have very regular design features. The upper and lower panels are nearly prismatic, the cross-sectional properties and the loading (axial compression) vary only slightly along the wing, while the rib supports are often equidistant, placed perpendicular to the principal direction of the loading. These particular characteristics offer a natural and practical way to simplify the analysis of these structures. The ''multi-bay panel model'' that is analyzed in this article is the outcome of this simplification.

The ''multi-bay panel model'' is a classical abstraction conceived for the study of the basic buckling characteristics of wing panels. It corresponds to a structure, where *a compression panel of the wing* (of length l), situated between two ribs, is imbedded on both ends in an infinitely long structure of panels of identical geometrical and material properties (Fig. 1). The infinite array of panels is, thus, simply supported on equidistant transverse ribs. The distance between the ribs l, equals the bay length of the panel in the actual wing box. The geometry and material properties of the cross-section, which are uniform over the length of the model are the averaged properties of the panel in the bay under investigation. This particular simplification has been the subject of numerous elaboration's in the past (van der Neut, 1952; Benthem, 1959; Przemieniecki, 1973; Wittrick et al., 1986), but to this day, the general solution still presents considerable difficulties.

0020-7683/00/$ - see front matter © 2000 Published by Elsevier Science Ltd.
PII: S0020-7683(99)00315-7

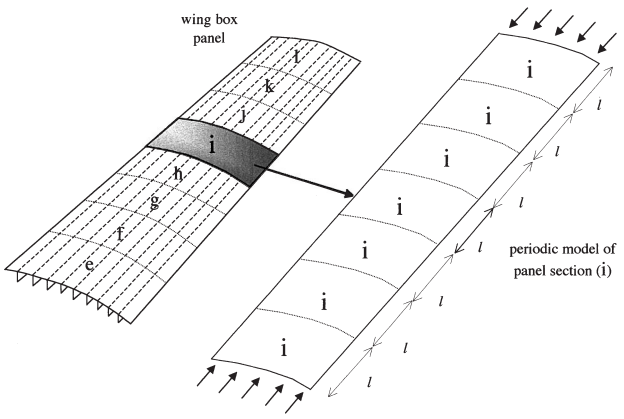

Fig. 1. The panel problem simplified.

1.2. General form of the solutions

The basic equilibrium state of the model corresponds to a uni-axial state of compression, which is (approximately) a linear function of the intensity of the applied load. Taking into account, the periodicity of the support conditions and the circumstance that the model is prismatic, the bifurcation buckling from this state must, in general, be governed by a bifurcation diagram of the pitchfork type (Fig. 2). In general, we mean here simple bifurcation as opposed to the particular case of bifurcation in multiple branches.

When buckling occurs with a buckling mode that is characterized by a wave pattern with a characteristic wave length equal or smaller than the bay length l, it is called local buckling. Local buckling in stiffened panels usually corresponds to a stable transition of state. In other words, the panel loading can be increased beyond the buckling load without immediate failure of the structure. This expectation follows from experience with the behavior of the type of structures under consideration here (Koiter, 1945; Budiansky, 1974).

Unstable buckling, generally, occurs if the wave length of the buckling mode in the axial direction coincides with two times the bay length l. In this case, the buckling phenomenon is called overall or global buckling. Unstable overall buckling can take place when the global mode is influenced by additional

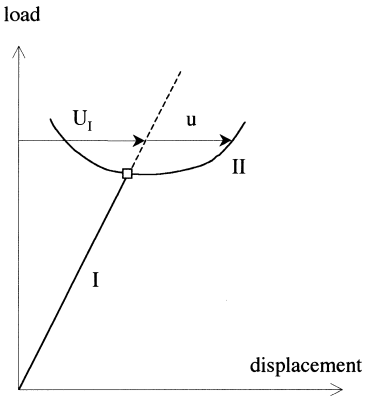

Fig. 2. Buckling as a bifurcation phenomenon.

stiffness reducing effects. These effects are for example, interaction with local modes, degradation of the material behavior during the onset of the buckling process (not considered here) or a detrimental additional deformation of the cross-section of the panels. An upper bound to the phenomenon of global buckling can be provided if the deformation of the cross-section is neglected and the longitudinal edge supports are not enforced. In that case, the behavior of the panel model is reduced to that of a beam on multiple supports and the buckling load then corresponds to the Euler load of a simply supported strut.

The method of solution discussed in this article is focused on a single mode bifurcation of the initial straight state of the panel. The multi-mode case is thus not considered here, although it can be developed on a similar basis. The method is a computerized application of Koiter's initial post-buckling theory (Koiter, 1970, 1976). Although approximate in nature, the solutions produced by it are expected to be acceptable in the range of load intensities within which the panels have to operate in practice. This observation especially refers to the local form of buckling. For the global form of buckling, the validity of the post-buckling solution may be somewhat more restricted.

1.3. The finite strip method

A general approach to the solution of the multi-bay problem is offered by nonlinear shell finite element codes such as STAGS (Rankin et al., 1989). However, this approach, which uses continuation methods (Riks, 1984), requires considerable power in computer resources. For computing the post-buckling stiffness in a preliminary design optimization procedure these programs are still too slow so that alternative approaches need be considered.

There are two ways to reduce the volume in computations. One is to replace the (two dimensional) finite element model of the panels by a (one dimensional) finite strip model, (Cheung, 1976), that exploits the periodicity present in the multi-bay panel. The other is to apply a perturbation method instead of a continuation procedure. Of course, the first choice introduces a rather severe limitation to the type of panels and loading conditions that can be admitted for analysis, while the second restricts the range of validity of the solutions. But the gain in speed by which the analyses can be carried out by the introduction of these choices is so significant that a code development on this basis can still be justified.

Successful computer implementations of the finite strip method for buckling analysis resulted, for example, in the codes BUCLASP (Vishwanatan and Tamakuni, 1973), and VIPASA (Wittrick and Williams, 1974; Plank and Wittrick, 1974). Another example of the code that employs the finite strip method is EMFTOR (van der Sloot, 1980). However, the capabilities of the first two are restricted to a *linearized buckling* analysis. This also counts for EMFTOR, although it has an added and special capability that aims at the prediction of the (ultimate) collapse state of the panel, which is associated with an overall mode triggered by non-linear material behavior. This particular extension will not be further discussed (van der Sloot, 1980).

Unfortunately, a *linearized buckling* analysis can neither provide an acceptable approximation of the post-buckling state, nor give an indication of the residual stiffness of the panel, once the load has exceeded the critical value. This is clearly a handicap. The knowledge of the post-buckling state is often important. Take for example the case, where the maximum load carrying capacity of the panel must be assessed on the basis of a limit state of the material in the post-buckling state (fracture in composites for example). The focus of this article is, therefore, on development of finite strip solution that *includes* the construction of the initial post-buckling terms. With this extension, the finite strip analysis as a quick, preliminary design tool will provide more information than was hitherto possible.

Graves-Smith and Shridharan (1981) were probably the first to demonstrate the possibilities of the finite strip approach to analyze the initial post-buckling behavior of prismatic plate structures. The author last mentioned developed the idea further in several follow up articles, (Shridharan and Graves-Smith, 1981; Shridharan, 1982, 1983; Shridharan and Ali, 1986), which clearly demonstrated the possibilities of this

approach. In the present article, the principal idea of the method is similar to that which was used by Graves-Smith and Shridharan. However, the development is completely independent, and unlike the work mentioned above, it is specifically geared here to the analysis of wing box panels by taking into account, the specific conditions that hold for these structures.

We finally mention that the work reported in this article was carried out in stages during the period 1983–1989. It was first described in Riks (1983, 1989) and Arendsen (1989), reports, which were not intended for general distribution. The resulting code, which we will refer to as PANBUCK in this article, is presently a part of the panel optimization code PANOPT developed by Arendsen (Arendsen and Wiggenraad, 1991; Arendsen, 1993).

2. Preliminary considerations

2.1. Basic conventions

Panels under consideration consist of an outer skin, which may be curved in the transverse direction but is straight in the axial (spanwise) direction. The skin is stiffened with thin walled members of the type sketched in Fig. 3. The stiffeners are bonded, riveted or are an integral part of the skin. Composite materials in the form of laminates can be used as long as the laminate build up meets certain symmetry requirements.

A panel will, thus, be conceived as an assembly of prismatic shell sections stretched out over the whole length ($2L = 2kl; k = \text{large}$) of the panel. While some of these sections are curved in the transverse direction, they will be modeled by subdividing them into plate finite elements of length $2L$ that are referred to as finite strips.

To describe the displacement of the plate strips, we introduce displacement functions defined with respect to orthogonal coordinate systems that are locally attached to the plate sections at some *reference* configuration of the panel. It is useful, at first, to let the reference configuration coincide with *the prebuckling state I*. We also use the convention that the plane $z = 0$ of the local coordinate systems coincide with the mid-surface of the plate strips.

When the base vectors of the local coordinate system are denoted by $\mathbf{e}_x$, $\mathbf{e}_y$, $\mathbf{e}_z$, the displacements of the mid-surface of the plate can be given as

$$\mathbf{u} = \mathbf{u}(x, y) = u(x, y)\mathbf{e}_x + v(x, y)\mathbf{e}_y + w(x, y)\mathbf{e}_z. \tag{2.1}$$

To describe the state of deformation of the plate elements, we introduce conventional small strain, small rotation (laminated) shell theory. This means that for the strain field, we use the Love/Kirchhoff assumption

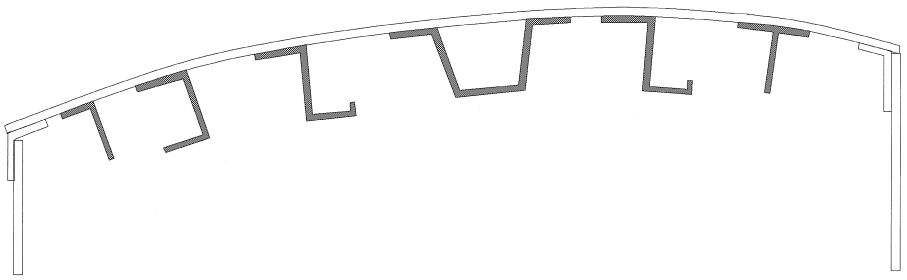

Fig. 3. Types of stiffeners.

$$\boldsymbol{\gamma}(\mathbf{u},z)=\boldsymbol{\varepsilon}(\mathbf{u})-z\boldsymbol{\kappa}(\mathbf{u}), \tag{2.2}$$

where, $\boldsymbol{\varepsilon}$ and $\boldsymbol{\kappa}$ correspond to the definitions of the membrane strains and the changes of the curvature of the mid-plane

$$\begin{aligned}
\varepsilon_{xx}&=\frac{\partial u}{\partial x}+\frac{1}{2}\left\{\left(\frac{\partial u}{\partial x}\right)^2+\left(\frac{\partial v}{\partial x}\right)^2+\left(\frac{\partial w}{\partial x}\right)^2\right\},\\
\varepsilon_{yy}&=\frac{\partial v}{\partial y}+\frac{1}{2}\left\{\left(\frac{\partial v}{\partial y}\right)^2+\left(\frac{\partial w}{\partial y}\right)^2+\left(\frac{\partial u}{\partial y}\right)^2\right\},\\
\varepsilon_{xy}&=\frac{1}{2}\left(\frac{\partial u}{\partial x}+\frac{\partial v}{\partial y}\right)+\frac{1}{2}\left\{\left(\frac{\partial u}{\partial x}\right)\left(\frac{\partial u}{\partial y}\right)+\left(\frac{\partial v}{\partial x}\right)\left(\frac{\partial v}{\partial y}\right)+\left(\frac{\partial w}{\partial x}\right)\left(\frac{\partial w}{\partial y}\right)\right\},
\end{aligned} \tag{2.3}$$

$$\begin{aligned}
\kappa_{xx}&=\frac{\partial^2 w}{\partial x^2},\\
\kappa_{yy}&=\frac{\partial^2 w}{\partial y^2},\\
\kappa_{xy}&=\frac{\partial^2 w}{\partial x\partial y}.
\end{aligned} \tag{2.4}$$

With these conventions, we can construct the potential energy functional that will stand at the basis of the development of the governing equations.

2.2. Potential energy

For small strains (Koiter, 1966, 1967), the increase of the elastic energy from state I to a neighboring state II is defined by

$$\begin{aligned}
V(\boldsymbol{\gamma})_{\mathrm{II}}-V(\mathbf{0})_{\mathrm{I}}&=\int_h\int_S\{W(\boldsymbol{\gamma})-W(\mathbf{0})\}\,\mathrm{d}z\,\mathrm{d}s,\\
V(\boldsymbol{\gamma})_{\mathrm{II}}-V(\mathbf{0})_{\mathrm{I}}&=\int_h\int_S\left\{\left\{\frac{\partial W}{\partial\boldsymbol{\gamma}}\right\}_{\mathrm{I}}\boldsymbol{\gamma}+\frac{1}{2}\left\{\frac{\partial^2 W}{\partial\boldsymbol{\gamma}\,\partial\boldsymbol{\gamma}}\right\}_{\mathrm{I}}\boldsymbol{\gamma}\boldsymbol{\gamma}+\mathrm{O}(\boldsymbol{\gamma}^3)\right\}\mathrm{d}z\,\mathrm{d}S.
\end{aligned} \tag{2.5}$$

W corresponds here to the specific elastic energy, and h, S denote that the integrals are taken over the thickness and reference surface, respectively. In this expression, the first derivative of the specific elastic energy W with respect to the strains can be identified as the prestress in the plate that from now on will be represented by the three component vector $\boldsymbol{\sigma}_{\mathrm{I}}=(\sigma_{xx},\,\sigma_{yy},\,\sigma_{xy})_{\mathrm{I}}^{\mathrm{T}}$. The second derivative of W corresponds to the matrix of elasticity constants. It will be denoted by $\mathbf{E}_{\mathrm{I}}$. Consequently, we write for Eq. (2.5)

$$V^*=V(\boldsymbol{\gamma})_{\mathrm{II}}-V(\mathbf{0})_{\mathrm{I}}=\int\int\boldsymbol{\sigma}_{\mathrm{I}}^{\mathrm{T}}(z)\boldsymbol{\gamma}\,\mathrm{d}z\,\mathrm{d}S+\int\int\boldsymbol{\gamma}^{\mathrm{T}}\mathbf{E}_{\mathrm{I}}(z)\boldsymbol{\gamma}\,\mathrm{d}z\,\mathrm{d}S. \tag{2.6}$$

As mentioned, all quantities including the integrals, are at this point defined with respect to the basic (pre-buckling) state I.

The *increase* of the total potential energy of the panel from state I to state II is then given by

$$P=V^*-\int_\Gamma\mathbf{T}^{\mathrm{T}}\mathbf{u}\,\mathrm{d}\Gamma. \tag{2.7}$$

The second term in the right-hand side is the work done by the external loading $\mathbf{T}$. The external loading consists of in-plane tractions acting along the boundaries Γ of the panel. In our case, this corresponds to the axial load distribution that is acting on the far ends $x = \pm L$. No other type of loading are considered here.

It follows that we can write

$$P = \int_h \int_S \boldsymbol{\sigma}_{\mathrm{I}}^{\mathrm{T}}(z)[\boldsymbol{\varepsilon} - z\boldsymbol{\kappa}]\,\mathrm{d}z\,\mathrm{d}S + \frac{1}{2}\int_h \int_S \boldsymbol{\varepsilon}^{\mathrm{T}}\mathbf{E}_{\mathrm{I}}(z)\boldsymbol{\varepsilon}\,\mathrm{d}z\,\mathrm{d}S + \int_h \int_S \boldsymbol{\varepsilon}^{\mathrm{T}}\mathbf{E}_{\mathrm{I}}(z)\boldsymbol{\kappa}z\,\mathrm{d}z\,\mathrm{d}S + \frac{1}{2}\int_h \int_S \boldsymbol{\kappa}^{\mathrm{T}}\mathbf{E}_{\mathrm{I}}(z)\boldsymbol{\kappa}z^2\,\mathrm{d}z\,\mathrm{d}S - \int_\Gamma \mathbf{T}^{\mathrm{T}}\mathbf{u}\,\mathrm{d}\Gamma. \tag{2.8}$$

The pre-buckling state I of the panel is assumed to be a uniform state of compression given by

$$\boldsymbol{\varepsilon}_{\mathrm{I}}^{\mathrm{T}} = (-\lambda\varepsilon_0, \lambda v_{12}(y)\varepsilon_0, 0)^{\mathrm{T}}, \qquad \boldsymbol{\kappa}_{\mathrm{I}} = 0, \tag{2.9}$$

where the parameter λ is the load intensity factor and ε_0 a nominal (reference) value of the axial strain at $\lambda = 1$. The component $\varepsilon_{xx} = -\lambda\varepsilon_0$ of the strain distribution in state I is equal and uniform in *all* parts of the panel. In the transverse direction, $\varepsilon_{yy} = \lambda v_{12}(y)\varepsilon_0$ may vary with y because the elasticity constant v_{12} of the laminate depends on the materials that are used for the various parts of the cross-section. These assumptions imply that the transverse stress σ_{yy} is neglected in state I, which is not unreasonable because, usually, the stiffener sections and outer skin in the wing box can expand freely in the transverse direction (except perhaps at the rib stations, an effect that we will ignore). Another consequence of the previous assumptions is that the theory developed here can only be applied to panels with a restricted choice of the laminate build-up. Laminates with bending–stretching coupling, for example, would in general show out-of-plane deformations at the very instant the load is applied [1] and this would violate our basic assumption about state I in (2.9).

With these restrictions, the third term in the right-hand side of Eq. (2.9) disappears so that the energy expression is reduced to

$$P = \int_h \int_S \boldsymbol{\sigma}_{\mathrm{I}}^{\mathrm{T}}(z)[\boldsymbol{\varepsilon} - z\boldsymbol{\kappa}]\,\mathrm{d}z\,\mathrm{d}S + \frac{1}{2}\int_h \int_S \boldsymbol{\varepsilon}^{\mathrm{T}}\mathbf{E}_{\mathrm{I}}(z)\boldsymbol{\varepsilon}\,\mathrm{d}z\,\mathrm{d}S + \frac{1}{2}\int_h \int_S \boldsymbol{\kappa}^{\mathrm{T}}\mathbf{E}_{\mathrm{I}}(z)\boldsymbol{\kappa}z^2\,\mathrm{d}z\,\mathrm{d}S - \int_\Gamma \mathbf{T}^{\mathrm{T}}\mathbf{u}\,\mathrm{d}\Gamma. \tag{2.10}$$

For convenience, we introduce the notation

$$\mathbf{N}_{\mathrm{I}}^{\mathrm{T}} = \int \boldsymbol{\sigma}_{\mathrm{I}}^{\mathrm{T}}(z)\,\mathrm{d}z \qquad \mathbf{C}_{\mathrm{I}} = \int \mathbf{E}_{\mathrm{I}}(z)\,\mathrm{d}z \qquad \mathbf{B}_{\mathrm{I}} = \int \mathbf{E}_{\mathrm{I}}(z)z^2\,\mathrm{d}z, \tag{2.11}$$

where

$\mathrm{N_I}$ is the vector of stress resultants in state I,

$\mathrm{C_I}$, the matrix of in-plane stiffnesses in state I and

$\mathrm{B_I}$, the matrix of bending stiffnesses in state I.

Expression (2.10) can then be written in the form:

$$P = \int_S \mathbf{N}_{\mathrm{I}}^{\mathrm{T}}\boldsymbol{\varepsilon}\,\mathrm{d}S + \frac{1}{2}\int_S \boldsymbol{\varepsilon}^{\mathrm{T}}\mathbf{C}_{\mathrm{I}}\boldsymbol{\varepsilon}\,\mathrm{d}S + \frac{1}{2}\int_S \boldsymbol{\kappa}^{\mathrm{T}}\mathbf{B}_{\mathrm{I}}\boldsymbol{\kappa}\,\mathrm{d}S - \int \mathbf{T}^{\mathrm{T}}\mathbf{u}\,\mathrm{d}\Gamma. \tag{2.12}$$

It is now expedient to write the vector of in-plane strains as the sum of two parts:

$$\boldsymbol{\varepsilon}(\mathbf{u}) = \mathbf{l}_1(\mathbf{u}) + \mathbf{l}_2(\mathbf{u}), \tag{2.13}$$

[1] In such cases, a bifurcation theory is not applicable unless the coupling is very weak. Please note, that for aerodynamic reasons, it is unlikely that laminates with strong stretching–bending coupling would be applied.

where $\mathbf{l}_1$ denotes the linear and $\mathbf{l}_2$ the quadratic form of $\boldsymbol{\varepsilon}$. Because the displacements $\mathbf{u}$ and the strain $\boldsymbol{\varepsilon}$ *are supposed to be measured with respect to state I*, a virtual displacement $\delta\mathbf{u}$ in the fundamental state I induces a virtual strain given by

$$\delta\boldsymbol{\varepsilon} = \boldsymbol{\varepsilon}(\delta\mathbf{u}) = \mathbf{l}_1(\delta\mathbf{u}). \tag{2.14}$$

This means that the fundamental state I must satisfy the variational equation:

$$\int \mathbf{N}_\mathrm{I}^\mathrm{T}\mathbf{l}_1\ (\delta\mathbf{u})\ \mathrm{d}S - \int \mathbf{T}^\mathrm{T}\,\delta\mathbf{u}\,\mathrm{d}\Gamma = 0. \tag{2.15a}$$

Consequently, if we substitute $\mathbf{u}$ for $\delta\mathbf{u}$ in Eq. (2.15a), the identity that results

$$\int \mathbf{N}_\mathrm{I}^\mathrm{T}\mathbf{l}_1(\mathbf{u})\,\mathrm{d}S - \int \mathbf{T}^\mathrm{T}\mathbf{u}\,\mathrm{d}\Gamma = 0 \tag{2.15b}$$

can be used to simplify Eq. (2.12) to

$$P = \int_S \mathbf{N}_\mathrm{I}^\mathrm{T}\mathbf{l}_2(\mathbf{u})\,\mathrm{d}S + \frac{1}{2}\int_S \boldsymbol{\varepsilon}^\mathrm{T}\mathbf{C}_\mathrm{I}\boldsymbol{\varepsilon}\,\mathrm{d}S + \frac{1}{2}\int_S \boldsymbol{\kappa}^\mathrm{T}\mathbf{B}_\mathrm{I}\boldsymbol{\kappa}\,\mathrm{d}S. \tag{2.16}$$

It is this functional that we will use as the starting point for all further considerations.

Remark: In the foregoing derivation, the prestress $\sigma_\mathrm{I}(z)$, or equivalently, the corresponding stress resultants $\mathbf{N}_\mathrm{I}$ of the pre-stress $\boldsymbol{\sigma}_\mathrm{I}(z)$ are supposed to be determined by $\boldsymbol{\varepsilon}_\mathrm{I}$ and thus are related to the (known) pre-buckling displacement field $\mathbf{U}_\mathrm{I} = \lambda\mathbf{U}_0$. Here, $\mathbf{U}_\mathrm{I}$ measures the difference between the pre-buckling state and the undeformed state. The field $\mathbf{u}$ is thus the shift from the pre-buckling state as defined in the decomposition

$$\mathbf{U}_\mathrm{total} = \lambda\mathbf{U}_0 + \mathbf{u} \tag{2.17}$$

with $\mathbf{U}_\mathrm{total}$ denoting the total displacement of the deformation incurred (Fig. 2). Throughout the remaining part of this article, this decomposition is further specified by the condition that both fields, $\mathbf{U}_\mathrm{I} = \lambda\mathbf{U}_0$ and $\mathbf{U}_\mathrm{total}$ are defined at the same value of the load (determined by the load factor λ).

3. Buckling equations

3.1. Simplification of the energy functional

We prefer to proceed here with a derivation of the perturbation equations that govern the buckling and post-buckling behavior of the panel model rather than taking them straightforwardly from the literature. This choice serves two purposes. In the first place, it seems appropriate to keep the development of the theory reasonably self contained for the benefit of those readers that are not quite familiar with the theory given in (Koiter, 1945; Budiansky, 1974). In the second place, such development offers the opportunity to stress the significance and limitations of the solutions that are produced by it. It is further noted that the treatment given here is directly focused on the construction of the bifurcation diagram of the panel model and is thus restricted to this particular case.

In the previous section, the basic equilibrium state I was taken as the reference state. We now observe that for the problem under discussion, the difference between the undeformed state 0 and the pre-buckling state I is expected to be very small. This means (Koiter, 1966) that it is permissible to ignore this difference

without serious consequences for the validity of expression (2.16) as the governing energy functional. [2] The formulation of Eq. (2.15) can thus further be simplified by evaluating the integrals with respect to the *undeformed state*. This also means that from now on we can drop the subscript I in the notation of the material constants $\mathbf{C}_I$, $\mathbf{B}_I$ and will write them as $\mathbf{C}$, $\mathbf{B}$.

With the decomposition of the membrane strains introduced in Eq. (2.13), the energy functional (2.16) can be ordered into polynomial form:

$$P(\mathbf{u};\lambda) = P_2^0(\mathbf{u}) - \lambda P_2'(\mathbf{u}) + P_3(\mathbf{u}) + P_4(\mathbf{u}), \tag{3.1}$$

where the terms in the right-hand side are given by

$$\begin{aligned} P_2^0(\mathbf{u}) &= \frac{1}{2}\int \mathbf{l}_1^{\mathrm{T}}(\mathbf{u})\mathbf{C}\mathbf{l}_1(\mathbf{u})\,\mathrm{d}S + \frac{1}{2}\int \boldsymbol{\kappa}_1^{\mathrm{T}}(\mathbf{u})\mathbf{B}\boldsymbol{\kappa}_1(\mathbf{u})\,\mathrm{d}S, \\ P_2'(\mathbf{u}) &= \int \mathbf{N}_0^{\mathrm{T}}\mathbf{l}_2(\mathbf{u})\,\mathrm{d}S, \end{aligned} \tag{3.2a}$$

$$P_3(\mathbf{u}) = \int \mathbf{l}_1^{\mathrm{T}}(\mathbf{u})\mathbf{C}\mathbf{l}_2(\mathbf{u})\,\mathrm{d}S, \tag{3.2b}$$

$$P_4(\mathbf{u}) = \frac{1}{2}\int \mathbf{l}_2^{\mathrm{T}}(\mathbf{u})\mathbf{C}\mathbf{l}_2(\mathbf{u})\,\mathrm{d}S. \tag{3.2c}$$

The parameter λ is the load intensity factor defined by

$$\mathbf{N}_I = -\lambda\mathbf{N}_0. \tag{3.3}$$

Here $\mathbf{N}_I$ is the vector of pre-buckling (membrane) stress resultants and $\mathbf{N}_0$ a reference value, which we can call the nominal load ($\mathbf{N}_0$ corresponds to the nominal axial strain ε_0). The notation adopted in Eqs. (3.1) and (3.2) is that which was introduced by Koiter (1945) and we will continue to use it in the sequel. See Appendix A for an explanation.

3.2. Governing equations in variational form

We will now derive the equilibrium equations for solutions other than the basic state $\mathbf{U}_I = \lambda\mathbf{U}_0$ in variational form. An arbitrary variation from the state $\mathbf{U}_{\mathrm{tot}} = \lambda\mathbf{U}_0 + \mathbf{u}$ is denoted by $\delta\mathbf{u} = \varepsilon\boldsymbol{\xi}$, where ε is a (non-vanishing) but arbitrarily small number and $\boldsymbol{\xi}$ is an arbitrary displacement function of the class of $\mathbf{u}$ (i.e. kinematically admissible). With this proposition, we can introduce the directional derivative of the functional P with respect to $\boldsymbol{\xi}$:

$$P_{\mathbf{u}}(\mathbf{u})\boldsymbol{\xi} = \frac{\mathrm{d}}{\mathrm{d}\varepsilon}\{P(\mathbf{u}+\varepsilon\boldsymbol{\xi})\} = \frac{\partial P(\mathbf{u})}{\partial\mathbf{u}}\boldsymbol{\xi} = \lim_{\varepsilon\to 0}\left\{\frac{P(\mathbf{u}+\varepsilon\boldsymbol{\xi}) - P(\mathbf{u})}{\varepsilon}\right\}. \tag{3.4}$$

The equilibrium states of the panel are determined by the stationary values of the potential energy Eq. (3.1). A stationary value of the potential energy is attained at a given state ($\mathbf{u}$, λ), if for any admissible $\boldsymbol{\xi}$ and any non-vanishing but arbitrarily small ε, the sign of the difference:

$$P(\mathbf{u}+\varepsilon\boldsymbol{\xi}) - P(\mathbf{u}) = [P_{\mathbf{u}}(\mathbf{u})\boldsymbol{\xi}]\varepsilon + \mathrm{O}(\varepsilon^2) \tag{3.5}$$

[2] It is far more laborious to arrive at Eqs. (3.1) and (3.2) when the undeformed state 0 is taken as reference configuration.

does not depend on the sign of ε. This means that

$$P_{\mathbf{u}}(\mathbf{u})\boldsymbol{\xi} = \lim_{\varepsilon \to 0}\left\{ \frac{P(\mathbf{u}+\varepsilon\boldsymbol{\xi}) - P(\mathbf{u})}{\varepsilon} \right\} = 0. \tag{3.6}$$

As can be verified, in terms of expansion (3.1), the limit given above corresponds to the (non-linear) variational equation:

$$P_{11}^{0}(\mathbf{u},\boldsymbol{\xi}) - \lambda P_{11}'(\mathbf{u},\boldsymbol{\xi}) + P_{21}(\mathbf{u},\boldsymbol{\xi}) + P_{31}(\mathbf{u},\boldsymbol{\xi}) = 0. \tag{3.7}$$

It is this equation, which determines all possible equilibrium states of the panel model (including the pre-buckling state $(\mathbf{u}, \lambda)_{\mathrm{I}} = (\mathbf{0}, \lambda)$), for any given value of the load. Eq. (3.7) (also referred to as the weak form of the governing equations) is equivalent to a set of (non-linear) partial-differential equations with boundary conditions, but the derivation of these equations is not of interest here.

3.3. Parametrization of the solutions

The solutions of Eq. (3.7) can be viewed as a family of curves in the space spanned by the displacement function $\mathbf{u}$ and the load parameter λ. In parametric form, any part of such a curve can be denoted by $(\mathbf{u}, \lambda) = \{\mathbf{u}(\eta), \lambda(\eta)\}$, where η stands for a suitable path parameter. The way to specify this parameter is to complement Eq. (3.7) with an extra equation:

$$\begin{aligned} &P_{11}^{0}(\mathbf{u},\boldsymbol{\xi}) - \lambda P_{11}'(\mathbf{u},\boldsymbol{\xi}) + P_{21}(\mathbf{u},\boldsymbol{\xi}) + P_{31}(\mathbf{u},\boldsymbol{\xi}) = 0, \\ &h(\mathbf{u},\lambda) - \eta = 0. \end{aligned} \tag{3.8}$$

Here $h(\mathbf{u}, \lambda)$ stands for a suitably chosen function of $\mathbf{u}$ and λ (Riks, 1984). A practical choice for $h(\mathbf{u}, \lambda)$ can be based on the following consideration. To measure the "length" of the displacement field $\mathbf{u}$, we introduce a positive definite quadratic form $T_2(\mathbf{u})$. This is an integral, which is built on the same arguments that appear in the quadratic forms $P_2^0(\mathbf{u})$ and/or $P_2'(\mathbf{u})$, but which is otherwise arbitrary (Koiter, 1945). (We will see that $P_2'(\mathbf{u})$ presents itself as a natural choice for T_2.) With this functional, we define the length of $\mathbf{u}$ by

$$\|\mathbf{u}\|^2 = T_2(\mathbf{u}) \quad \text{or} \quad \|\mathbf{u}\| = \sqrt{T_2(\mathbf{u})}. \tag{3.9}$$

Using the same functional, we consider the angle between two arbitrarily chosen fields $\mathbf{u}$, $\mathbf{v}$ to be defined by

$$\cos\theta = \frac{\frac{1}{2}T_{11}(\mathbf{u},\mathbf{v})}{\|\mathbf{u}\|\|\mathbf{v}\|}. \tag{3.10}$$

In this expression, T_{11} is the bilinear form that arises in the (binomial) expansion of T_2:

$$T_2(\mathbf{u}+\mathbf{v}) = T_2(\mathbf{u}) + T_{11}(\mathbf{u},\mathbf{v}) + T_2(\mathbf{v}). \tag{3.11}$$

With Eq. (3.10), we introduce an inner product rule and it follows from this definition that $\mathbf{u}$ is declared to be orthogonal to $\mathbf{v}$ if

$$T_{11}(\mathbf{u},\mathbf{v}) = 0. \tag{3.12}$$

Our principal interest goes out to the particular solution of Eq. (3.8) that branches off the pre-buckling state I at the smallest positive value of the load $\lambda = \lambda_{\mathrm{c}}$. To examine where this occurs, we will consider the Taylor expansion of the basic state I developed at an arbitrary point: $\{\mathbf{U}_1, \lambda_1\} = \{\lambda_1\mathbf{U}_0, \lambda_1\}$. Notice that in terms of the additional displacement this corresponds to $\{\mathbf{u}_1, \lambda_1\} = \{\mathbf{0}, \lambda_1\}$. Without loss of generality, it can be assumed that at $\{\mathbf{u}_1, \lambda_1\}$, $\eta = 0$, so that the Taylor expansion of the solution $\{\mathbf{u}(\eta), \lambda(\eta)\}$ around $\{\mathbf{u}_1, \lambda_1\}$ is given by

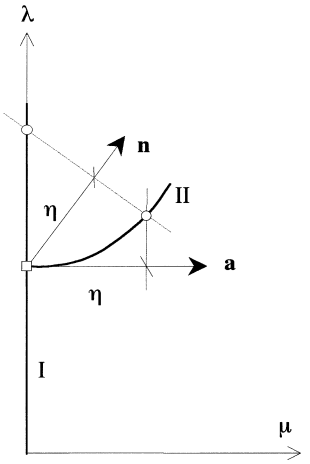

Fig. 4. Perturbation parameter choices.

$$\begin{aligned}\mathbf{u}(\eta)-\mathbf{u}_1&=\overset{\circ}{\mathbf{u}}_1\eta+\tfrac{1}{2}\overset{\circ\circ}{\mathbf{u}}_1\eta^2+\cdots+,\\ \lambda(\eta)-\lambda_1&=\overset{\circ}{\lambda}_1\eta+\tfrac{1}{2}\overset{\circ\circ}{\lambda}_1\eta^2+\cdots+.\end{aligned}\tag{3.13}$$

Here differentiation with respect to η is denoted by

$$\frac{\mathrm{d}(\ )}{\mathrm{d}\eta}=(^{\circ});\qquad \frac{\mathrm{d}^2(\ )}{\mathrm{d}\eta^2}=(^{\circ\circ}),\qquad \overset{\circ}{\mathbf{u}}_1=\overset{\circ}{\mathbf{u}}(0);\qquad \overset{\circ}{\lambda}_1=\overset{\circ}{\lambda}(0),\ \text{etc.}$$

We will now choose the parameter η by specifying equation $h(\mathbf{u},\lambda)-\eta=0$ as

$$\tfrac{1}{2}T_{11}(\mathbf{n},\Delta\lambda\mathbf{U}_0+\mathbf{u})-\eta=0.\tag{3.14}$$

In this form $\Delta\lambda$ is given by $\Delta\lambda=\lambda-\lambda_1$ and $\mathbf{n}$ is an arbitrary vector (field) of unit length that we can choose in any appropriate way, i.e., in a way that suits the analysis as best as possible. We note that in this manner the path parameter η is locally defined, that is, it is defined with respect to the solution $\{\mathbf{U}_1,\ \lambda_1\}$ at which expansion (3.13) is evaluated. The geometrical significance of the use of Eq. (3.14) is illustrated in Fig. 4.

3.4. The perturbation equations

We will now consider expansion (3.13) as the solution for the branch of the first bifurcation point along I:$\{\lambda\mathbf{U}_0,\lambda\}$. Our incentive is to compute the first two terms of Eq. (3.13). The equations that determine the path derivatives $(\overset{\circ}{\mathbf{u}}_1,\overset{\circ}{\lambda}_1)$, $(\overset{\circ\circ}{\mathbf{u}}_1,\overset{\circ\circ}{\lambda}_1),\ldots,$ at $(\mathbf{u}_1,\ \lambda_1)$ are obtained by successive differentiation of Eq. (3.7) and the auxiliary Eq. (3.14) with respect to η. It leads to the sequence of equations:

$$P^0_{11}(\overset{\circ}{\mathbf{u}}_1,\boldsymbol{\xi})-\lambda_1P'_{11}(\overset{\circ}{\mathbf{u}}_1,\boldsymbol{\xi})-\overset{\circ}{\lambda}_1P'_{11}(\mathbf{u}_1,\boldsymbol{\xi})+P_{111}(\mathbf{u}_1,\overset{\circ}{\mathbf{u}}_1,\boldsymbol{\xi})+P_{211}(\mathbf{u}_1,\overset{\circ}{\mathbf{u}}_1,\boldsymbol{\xi})=0,\tag{3.15a}$$

$$\tfrac{1}{2}T_{11}(\mathbf{n},\overset{\circ}{\lambda}_1\mathbf{U}_0+\overset{\circ}{\mathbf{u}}_1)-1=0,\tag{3.15b}$$

$$\begin{aligned}&P^0_{11}(\overset{\circ\circ}{\mathbf{u}}_1,\boldsymbol{\xi})-\lambda_1P'_{11}(\overset{\circ\circ}{\mathbf{u}}_1,\boldsymbol{\xi})-\overset{\circ\circ}{\lambda}_1P'_{11}(\mathbf{u}_1,\boldsymbol{\xi})-2\overset{\circ}{\lambda}_1P'_{11}(\overset{\circ}{\mathbf{u}}_1,\boldsymbol{\xi})+P_{111}(\overset{\circ}{\mathbf{u}}_1,\overset{\circ}{\mathbf{u}}_1,\boldsymbol{\xi})+P_{111}(\mathbf{u}_1,\overset{\circ\circ}{\mathbf{u}}_1,\boldsymbol{\xi})\\&\quad+P_{1111}(\mathbf{u}_1,\overset{\circ}{\mathbf{u}}_1,\overset{\circ}{\mathbf{u}}_1,\boldsymbol{\xi})+P_{211}(\mathbf{u}_1,\overset{\circ\circ}{\mathbf{u}}_1,\boldsymbol{\xi})=0,\end{aligned}\tag{3.16a}$$

$$\tfrac{1}{2}T_{11}(\mathbf{n}, \overset{\circ\circ}{\lambda}_1\mathbf{U}_0 + \overset{\circ\circ}{\mathbf{u}}_1) = 0, \tag{3.16b}$$

$$P^0_{11}(\overset{\circ\circ\circ}{\mathbf{u}}_1, \boldsymbol{\xi}) - \lambda_1 P'_{11}(\overset{\circ\circ\circ}{\mathbf{u}}_1, \boldsymbol{\xi}) - 3\overset{\circ\circ}{\lambda}_1 P'_{11}(\overset{\circ}{\mathbf{u}}_1, \boldsymbol{\xi}) - 3\overset{\circ}{\lambda}_1 P'_{11}(\overset{\circ\circ}{\mathbf{u}}_1, \boldsymbol{\xi}) - \overset{\circ\circ\circ}{\lambda}_1 P'_{11}(\mathbf{u}_1, \boldsymbol{\xi}) + 3P_{111}(\overset{\circ}{\mathbf{u}}_1, \overset{\circ\circ}{\mathbf{u}}_1, \boldsymbol{\xi}) + P_{111}(\mathbf{u}_1, \overset{\circ\circ\circ}{\mathbf{u}}_1, \boldsymbol{\xi}) + P_{1111}(\overset{\circ}{\mathbf{u}}_1, \overset{\circ}{\mathbf{u}}_1, \overset{\circ}{\mathbf{u}}_1, \boldsymbol{\xi}) + 3P_{1111}(\mathbf{u}_1, \overset{\circ}{\mathbf{u}}_1, \overset{\circ\circ}{\mathbf{u}}_1, \boldsymbol{\xi}) + P_{211}(\mathbf{u}_1, \overset{\circ\circ\circ}{\mathbf{u}}_1, \boldsymbol{\xi}) = 0, \tag{3.17a}$$

$$\tfrac{1}{2}T_{11}(\mathbf{n}, \overset{\circ\circ\circ}{\lambda}_1\mathbf{U}_0 + \overset{\circ\circ\circ}{\mathbf{u}}_1) = 0, \tag{3.17b}$$

etc. We note that the third-order set of Eqs. (3.17a) and (3.17b) is included here because, as it will transpire, it is otherwise not possible to complete the solution for $\overset{\circ\circ}{\lambda}_1$.

It is now, the time to particularize Eqs. (3.15)–(3.17) to the case that $\{\mathbf{u}_1, \lambda_1\}$ corresponds to a solution of the pre-buckling state I, so that $\{\mathbf{u}_1, \lambda_1\} = \{\mathbf{0}, \lambda_1\}$. For convenience, we introduce a simplification in the auxiliary equations by demanding that $\mathbf{n}$ is orthogonal to $\mathbf{U}_0$, i.e., $T_{11}(\mathbf{n}, \mathbf{U}_0) = 0$. Finally, we will drop the subscript $(\,)_1$ because carrying it about is not really necessary in what follows. The result of these changes is

$$P^0_{11}(\overset{\circ}{\mathbf{u}}, \boldsymbol{\xi}) - \lambda P'_{11}(\overset{\circ}{\mathbf{u}}, \boldsymbol{\xi}) = 0, \tag{3.18a}$$

$$\tfrac{1}{2}T_{11}(\mathbf{n}, \overset{\circ}{\mathbf{u}}) - 1 = 0, \tag{3.18b}$$

$$P^0_{11}(\overset{\circ\circ}{\mathbf{u}}, \boldsymbol{\xi}) - \lambda P'_{11}(\overset{\circ\circ}{\mathbf{u}}, \boldsymbol{\xi}) - 2\overset{\circ}{\lambda} P'_{11}(\overset{\circ}{\mathbf{u}}, \boldsymbol{\xi}) + P_{111}(\overset{\circ}{\mathbf{u}}, \overset{\circ}{\mathbf{u}}, \boldsymbol{\xi}) = 0, \tag{3.19a}$$

$$\tfrac{1}{2}T_{11}(\mathbf{n}, \overset{\circ\circ}{\mathbf{u}}) = 0, \tag{3.19b}$$

$$P^0_{11}(\overset{\circ\circ\circ}{\mathbf{u}}, \boldsymbol{\xi}) - \lambda P'_{11}(\overset{\circ\circ\circ}{\mathbf{u}}, \boldsymbol{\xi}) - 3\overset{\circ\circ}{\lambda} P'_{11}(\overset{\circ}{\mathbf{u}}, \boldsymbol{\xi}) - 3\overset{\circ}{\lambda} P'_{11}(\overset{\circ\circ}{\mathbf{u}}, \boldsymbol{\xi}) + 3P_{111}(\overset{\circ}{\mathbf{u}}, \overset{\circ\circ}{\mathbf{u}}, \boldsymbol{\xi}) + P_{1111}(\overset{\circ}{\mathbf{u}}, \overset{\circ}{\mathbf{u}}, \overset{\circ}{\mathbf{u}}, \boldsymbol{\xi}) = 0, \tag{3.20}$$

$$\tfrac{1}{2}T_{11}(\mathbf{n}, \overset{\circ\circ\circ}{\mathbf{u}}) = 0.$$

These equations determine the path derivatives of the basic state I at any value of λ. The question of a possible bifurcation hinges on the question of the uniqueness of the solutions of Eqs. (3.18)–(3.20). Because we derived these equations along the basic state I, we know and can verify that $\overset{\circ}{\mathbf{u}} = \mathbf{0}, \overset{\circ\circ}{\mathbf{u}} = \mathbf{0}, \overset{\circ\circ\circ}{\mathbf{u}} = \mathbf{0}$, etc. is always a solution. This (trivial) solution corresponds to the expansion of the pre-buckling state I. But the presence of *any* other *non-zero* solution for $\overset{\circ}{\mathbf{u}}, \overset{\circ\circ}{\mathbf{u}}$ etc. at a particular value $\lambda = \lambda_1$ signifies a loss of uniqueness of the solutions for the path derivatives at $\{\mathbf{0}, \lambda_1\}$and thus represents a bifurcation from I at this point. Therefore, Eqs. (3.18)–(3.20) determine also the path derivatives of an equilibrium path II that branches off the basic state I.

3.5. The (initial) buckling equations

It is necessary to discuss first, the solution of Eqs. (3.18a) and (3.18b). The variational Eq. (3.18a) of this system is homogeneous in $\overset{\circ}{\mathbf{u}}$. It can only have non-zero solutions $\overset{\circ}{\mathbf{u}} = \mathbf{a}_i$ for special values of $\lambda = \lambda_i$ $(i = 1, 2, 3, \ldots)$. This eigenvalue problem determines the locations of bifurcation points along the basic state I and provides information about the directions of the bifurcations at the bifurcation points determined by λ_i, in terms of the eigenmodes or buckling modes $\mathbf{a}_i$. But only the first bifurcation point $\{\mathbf{0}, \lambda_c\}$ determined

by the lowest eigenvalue $\lambda_c = \lambda_1 \leqslant \lambda_i$, is of interest here, because it is at this particular point that the panel will undergo a change from state I into another state II.

The lowest eigenvalue λ_c is called the (critical) buckling load and the corresponding solution for the displacement field $\overset{\circ}{\mathbf{u}} = \mathbf{a}_c$ is called the (critical) buckling mode. Bifurcations of the solutions that occur along the unstable part of $(\mathbf{0}, \lambda)_I$ at values of $\lambda_i > \lambda_c$ are not of any relevance for the physical behavior of the panel (unless λ_i are close to λ_c) and are therefore not considered here.

Eqs. (3.18) have some special properties that play an important role in the theory, so that we summarize them below. It follows from the symmetry of the bi-linear forms in Eq. (3.17a)

$$P^0_{11}(\mathbf{u},\mathbf{v}) = \int \mathbf{l}^{\mathrm{T}}_1(\mathbf{u})\mathbf{C}\mathbf{l}_1(\mathbf{v})\,\mathrm{d}S + \int \boldsymbol{\kappa}^{\mathrm{T}}_1(\mathbf{u})\mathbf{B}\boldsymbol{\kappa}_1(\mathbf{v})\,\mathrm{d}S = P^0_{11}(\mathbf{v},\mathbf{u}),$$

$$P'_{11}(\mathbf{u},\mathbf{v}) = \int \mathbf{N}^{\mathrm{T}}_0\mathbf{l}_{11}(\mathbf{u},\mathbf{v})\,\mathrm{d}S = P'_{11}(\mathbf{v},\mathbf{u})$$

that the solutions λ_i, $\mathbf{a}_i$ for $\lambda_i \neq \lambda_j$, $(i \neq j)$ satisfy the property:

$$P^0_{11}(\mathbf{a}_i,\mathbf{a}_j) = P'_{11}(\mathbf{a}_i,\mathbf{a}_j) = 0. \tag{3.21}$$

This means that the eigenmodes are orthogonal with respect to the bilinear forms given above. Because Eq. (3.18a) is homogenous, the solutions are only determined apart from a constant. The constant is determined by the second (scalar) Eq. (3.18b). Its value depends on the choice of T_2 and $\mathbf{n}$. If we take the admissible choice $T_2 = P'_2(\mathbf{u})$, and set $\mathbf{n} = \overset{\circ}{\mathbf{u}}$, system (3.18) is changed to

$$\begin{aligned} &P^0_{11}(\overset{\circ}{\mathbf{u}},\boldsymbol{\xi}) - \lambda P'_{11}(\overset{\circ}{\mathbf{u}},\boldsymbol{\xi}) = 0,\\ &\tfrac{1}{2}P'_{11}(\overset{\circ}{\mathbf{u}},\overset{\circ}{\mathbf{u}}) - 1 = 0. \end{aligned} \tag{3.22}$$

This set of equations has the same solutions as Eq. (3.18a) and (3.18b)

$$\overset{\circ}{\mathbf{u}} = \mathbf{a}_i, \quad \lambda = \lambda_i \ (i = 1,2,3,4,5,\ldots),$$

which for $\lambda_i \neq \lambda_j$, $j \neq i$, satisfy the relations:

$$\tfrac{1}{2}P'_{11}(\mathbf{a}_i,\mathbf{a}_j) = \delta_{ij} \qquad \tfrac{1}{2}P^0_{11}(\mathbf{a}_i,\mathbf{a}_j) = \lambda_i\delta_{ij}\,(\text{no sum over } i) \tag{3.23}$$

$$(\delta_{ij} = \text{Kronecker delta})\ (i,j = 1,2,3,4,\ldots).$$

We observe that the choices $T_2(\mathbf{u}) = P'_2(\mathbf{u})$ and $\mathbf{n} = \overset{\circ}{\mathbf{u}}$ lead to a compact and convenient formulation. In the following, we will concentrate on the solutions that are determined by $\mathbf{a}_1 = \mathbf{a}_c$ and, accordingly, take for $\mathbf{n}$ the "direction" $\mathbf{n} = \mathbf{a}_c$.

3.6. The second-order terms

It will now be assumed that the solution of Eq. (3.22), i.e., the critical buckling load $\lambda_1 = \lambda_c$ and corresponding mode $\mathbf{a}_1 = \mathbf{a}_c$ have been determined. The unknowns that are still to be determined are $\overset{\circ}{\lambda}_{II}$ and the pair $\{\overset{\circ\circ}{\mathbf{u}}, \overset{\circ\circ}{\lambda}_{II}\}$. The subscript II attached to $\overset{\circ}{\lambda}$ and $\overset{\circ\circ}{\lambda}$ emphasize that just as $\overset{\circ\circ}{\mathbf{u}}$, these quantities belong to the branch II (Fig. 2). The continuation of the analysis begins with the second-order system (3.19). With the changes in notation and the new information obtained by the solution of Eq. (3.22), this system can be written as:

$$P^0_{11}(\overset{\circ\circ}{\mathbf{u}},\boldsymbol{\xi}) - \lambda_c P'_{11}(\overset{\circ\circ}{\mathbf{u}},\boldsymbol{\xi}) - 2\overset{\circ}{\lambda}_{II}P'_{11}(\mathbf{a}_c,\boldsymbol{\xi}) + P_{111}(\mathbf{a}_c,\mathbf{a}_c,\boldsymbol{\xi}) = 0, \tag{3.24a}$$

$$\tfrac{1}{2}P'_{11}(\mathbf{a}_c, \overset{\circ\circ}{\mathbf{u}}) = 0. \tag{3.24b}$$

Eq. (3.24a) is linear and inhomogeneous. The solution $\overset{\circ\circ}{\mathbf{u}}$ is subject to the side condition (3.24b) that requires $\overset{\circ\circ}{\mathbf{u}}$ to be orthogonal to $\mathbf{a}_c$. But the variational Eq. (3.24a) must hold for any admissible function $\boldsymbol{\xi}$ not necessarily perpendicular to $\mathbf{a}_c$. It should thus also hold for $\boldsymbol{\xi} = \mathbf{a}_c$. Substitution of this particular choice in (3.24a) and using $P'_{11}(\mathbf{a}_c, \overset{\circ\circ}{\mathbf{u}}) = P^0_{11}(\mathbf{a}_c, \overset{\circ\circ}{\mathbf{u}}) = 0$ leads to the identity:

$$\overset{\circ}{\lambda}_{cII} = \frac{P_{111}(\mathbf{a}_c, \mathbf{a}_c, \mathbf{a}_c)}{4P'_2(\mathbf{a}_c)} = \frac{3P_3(\mathbf{a}_c)}{2P'_2(\mathbf{a}_c)} = \frac{3}{2}P_3(\mathbf{a}_c). \tag{3.25}$$

It is noted that this condition (3.25), which determines $\overset{\circ}{\lambda}$ can be interpreted as a compatibility condition for the solution of system (3.24a) and (3.24b).

It is a consequence of the periodicity of the solutions in axial direction that the multi-bay problem is always governed by a *symmetric bifurcation point*. In that case, we can show that $P(\mathbf{u}(\eta)) = P(\mathbf{u}(-\eta))$ and this implies that $P_3(\mathbf{a}_c) \equiv 0$ and consequently $\overset{\circ}{\lambda}_{cII} \equiv 0$. The term $\overset{\circ}{\lambda}_{cII} P_{11}{}'(\mathbf{a}_c, \boldsymbol{\xi})$ can thus be dropped in Eqs. (3.24a) and (3.24b). A further discussion about the solution of the system Eqs. (3.24a) and (3.24b) is not necessary at this point. Some particular aspects of it will be considered later. It will, here, be simply assumed that the solution of Eqs. (3.24a) and (3.24b) $\mathbf{v} = \overset{\circ\circ}{\mathbf{u}}$ can be obtained as soon $\mathbf{a}_c$ is determined. This leads us then to the discussion of the computation of the last undetermined quantity, the derivative $\overset{\circ\circ}{\lambda}_{II}$. The curvature term $\overset{\circ\circ}{\lambda}_{II}$ does not appear in Eq. (3.19), but in the third-order derivative Eq. (3.20). With the information obtained so far Eq. (3.20) can be simplified to

$$P^0_{11}(\overset{\circ\circ\circ}{\mathbf{u}}, \boldsymbol{\xi}) - \lambda_c P'_{11}(\overset{\circ\circ\circ}{\mathbf{u}}, \boldsymbol{\xi}) - 3\overset{\circ\circ}{\lambda}_{cII} P'_{11}(\mathbf{a}_c, \boldsymbol{\xi}) + 3P_{111}(\mathbf{a}_c, \overset{\circ\circ}{\mathbf{u}}, \boldsymbol{\xi}) + P_{1111}(\mathbf{a}_c, \mathbf{a}_c, \mathbf{a}_c, \boldsymbol{\xi}) = 0, \tag{3.26a}$$

$$\tfrac{1}{2}P'_{11}(\mathbf{a}_c, \overset{\circ\circ\circ}{\mathbf{u}}) = 0. \tag{3.26b}$$

Note the $\overset{\circ\circ}{\mathbf{u}}$ in this expression is determined by Eqs. (3.24a) and (3.24b). Just as in the previous case also Eq. (3.26a) must be satisfied for all kinematically admissible variations $\boldsymbol{\xi}$. This yields as compatibility condition ($\boldsymbol{\xi} = \mathbf{a}_c$):

$$\overset{\circ\circ}{\lambda}_{cII} = \frac{1}{6P'_2(\mathbf{a}_c)}[3P_{111}(\mathbf{a}_c, \mathbf{a}_c, \overset{\circ\circ}{\mathbf{u}}) + P_{1111}(\mathbf{a}_c, \mathbf{a}_c, \mathbf{a}_c, \mathbf{a}_c)] = \frac{1}{P'_2(\mathbf{a}_c)}[4P_4(\mathbf{a}_c) + 6P_{21}(\mathbf{a}_c, \overset{\circ\circ}{\mathbf{u}})]$$

or, with $P_2(\mathbf{a}_c) = 1$, and the identity: $\{P^0_2(\overset{\circ\circ}{\mathbf{u}}) - \lambda_c P'_2(\overset{\circ\circ}{\mathbf{u}})\} = -P_{21}(\mathbf{a}_c, \overset{\circ\circ}{\mathbf{u}})$ that follows when we substitute $\xi = \overset{\circ\circ}{\mathbf{u}}$ in Eq. (3.24a),

$$\overset{\circ\circ}{\lambda}_{cII} = 4P_4(\mathbf{a}_c) - \{P^0_2(\overset{\circ\circ}{\mathbf{u}}) - \lambda_c P'_2(\overset{\circ\circ}{\mathbf{u}})\}. \tag{3.27}$$

Expressions (3.25) and (3.27) correspond to the classical results obtained by Koiter (1945).

The final solution to the panel problem can now be written as

$$\mathbf{u}(\eta) = \mathbf{a}_c\eta + \tfrac{1}{2}\mathbf{v}\eta^2, \tag{3.28a}$$

$$\lambda(\eta) = \lambda_c + \tfrac{1}{2}\overset{\circ\circ}{\lambda}_{cII}\eta^2, \tag{3.28b}$$

where the buckling mode $\mathbf{a}_c$ is determined by Eq. (3.22) and the first correction term $\mathbf{v} = \overset{\circ\circ}{\mathbf{u}}$ is the solution for Eqs. (3.24a) and (3.24b). Please note that the path parameter η in (3.28a) can be seen as the component of the buckling mode $\mathbf{a}_c$ in the field $\mathbf{u}$. The term $(1/2)\eta^2\mathbf{v}$ is thus the orthogonal complement to $\eta\mathbf{a}_c$ in $\mathbf{u}$.

3.7. The fundamental bifurcation equation

The functional relationship (3.28b) between the load parameter λ and the path parameter η has a special significance that can be understood by the following consideration. The equilibrium equations in unabridged form are given by Eq. (3.7):

$$P_{11}(\mathbf{u},\boldsymbol{\xi}) + P_{21}(\mathbf{u},\boldsymbol{\xi}) + P_{31}(\mathbf{u},\boldsymbol{\xi}) = 0, \tag{3.29a}$$

with

$$P_{11}(\mathbf{u},\boldsymbol{\xi}) = P^0_{11}(\mathbf{u},\boldsymbol{\xi}) - \lambda P'_{11}(\mathbf{u},\boldsymbol{\xi}) \tag{3.29b}$$

and $\boldsymbol{\xi}$ is any admissible variation of $\mathbf{u}$. We now take a special 'direction' for $\boldsymbol{\xi}$, i.e., $\boldsymbol{\xi} = \mathbf{a}_c$ thus projecting Eqs. (3.29a) and (3.29b) to $\mathbf{a}_c$ and substitute Eq. (3.28a) for the solution $\mathbf{u}$. After some manipulation and the use of the identities: $\lambda_{cII} = 0$, $P^0_2(\mathbf{a}_c) - \lambda_c P'_2(\mathbf{a}_c) = 0$ and $P_2(\mathbf{v}) + P_{21}(\mathbf{a}_c, \mathbf{v}) = 0$, we obtain

$$-2(\lambda - \lambda_c)P'_2(\mathbf{a}_c)\eta + 4\{P_4(\mathbf{a}_c) - \tfrac{1}{4}[P^0_2(\mathbf{v}) - \lambda P'_2(\mathbf{v})]\}\eta^3 + O(\eta^4) = 0. \tag{3.30}$$

This *single* equation represents an equilibrium equation in terms of λ and η and it describes the bifurcation phenomenon in condensed form. It follows that the solution of Eq. (3.30) can be separated in two parts:

$$\begin{aligned} &(i) \quad \eta = 0 \quad \rightarrow \text{ the fundamental state I,} \\ &(ii) \quad 2(\lambda - \lambda_c) - \overset{\circ\circ}{\lambda}_{cII}\eta^2 = 0 \quad \rightarrow \text{ the post-buckling state II} \end{aligned} \tag{3.31}$$

and we notice that the last result (ii) turns out to be identical to (3.28b). Thus the cardinal part of the solution, which takes place in the subspace spanned by (η, λ) (the direction of the buckling mode and λ), is represented by Eq. (3.28b).

4. The spatial form of the solutions

4.1. The buckling modes

In this section, we will introduce the global form of the differential equations with periodicity conditions that are equivalent to the variational equations given by Eqs. (3.18)–(3.20). This is done in order to facilitate the discussion of the *selection* of the appropriate solutions in the axial direction. But because the finite strip method directly solves the variational equations rather than the differential equations, it is not necessary to present the latter in more detail than is strictly necessary for our discussion.

Thus, just as Eqs. (3.7), (3.18)–(3.20) can be converted to systems of partial differential equations with boundary conditions. Symbolically, we can write the equations that correspond to Eqs. (3.18)–(3.20) as

$$\begin{aligned} &\mathbf{D}^0_1(\overset{\circ}{\mathbf{u}}) - \lambda \mathbf{D}'_1(\overset{\circ}{\mathbf{u}}) = 0 \\ &\qquad\qquad + \text{ boundary conditions} \\ &P'_{11}(\overset{\circ}{\mathbf{u}}, \overset{\circ}{\mathbf{u}}) - 1 = 0, \end{aligned} \tag{4.1}$$

$$\begin{aligned} &\mathbf{D}^0_1(\overset{\circ\circ}{\mathbf{u}}) - \lambda \mathbf{D}'_1(\overset{\circ\circ}{\mathbf{u}}) = \mathbf{D}^1_2(\overset{\circ}{\mathbf{u}}) \\ &\qquad\qquad + \text{ boundary conditions} \\ &P'_{11}(\overset{\circ}{\mathbf{u}}, \overset{\circ\circ}{\mathbf{u}}) = 0, \end{aligned} \tag{4.2}$$

where $\mathbf{D}^0_1$, $\mathbf{D}^1_1$ denote two linear homogeneous differential operators and $\mathbf{D}^1_2$ denotes a non-linear differential operator of the degree 2. For the prediction of the axial shape of the solutions of Eqs. (4.1) and (4.2), we

only need to focus on the formulation of the boundary conditions and the global form of the right-hand side of Eq. (4.2).

The conditions along the longitudinal edges of the panel generally correspond to that of simple support, and as we will see later, the finite strip method will allow us to satisfy the kinematic part of these conditions exactly. However, there are also support conditions to be fulfilled at the rib situations: $x = \pm kl$, for $k = 1$, 2, 3, 4, 5,... These support conditions are determined by the way the compression panels are fastened to the ribs. In most wing box designs, the fastening is restricted to the skin of the panel, and does not include the stiffeners. We will therefore assume that the support conditions at the rib stations correspond to the suppression of w at $x = \pm kl$.

The first set of partial differential Eq. (4.1), equivalent to Eq. (3.18a), yields the eigen solutions:

$$\overset{\circ}{\mathbf{u}} = \mathbf{a_i} \quad \lambda = \lambda_\mathbf{i} \qquad \text{for } i = c, 2, 3, 4, 5 \ldots \tag{4.3}$$

with the property that all eigenmodes are real and all eigenvalues are positive. Just as in the previous section, it is assumed that sequence (4.3) is ordered in the following way: $\lambda_c < \lambda_2 \leqslant \cdots \leqslant \lambda_n \leqslant \cdots$ As before, we discuss the simplest case, i.e. when λ_c is well separated from the other characteristic values $\lambda_i : i = 2$, 3,....

Because the panel model is periodic in axial direction, we can use the following particular solutions for Eq. (4.1)

$$\overset{\circ}{\mathbf{u}}_c = \mathbf{a}_c = \begin{Bmatrix} u(x,y) \\ v(x,y) \\ w(x,y) \end{Bmatrix} = \begin{Bmatrix} h(y)\cos px \\ g(y)\sin px \\ f(y)\sin px \end{Bmatrix}, \tag{4.4}$$

where the wave number p is given by $p = m\pi/l$; $m = 1, 2, 3, 4, 5, \ldots$ Note, that at $x = \pm(kl)$, $k = 1, 2, 3, 4, \ldots$, functions (4.4) take the values:

$$\overset{\circ}{\mathbf{u}}_c = \begin{pmatrix} \overset{\circ}{u}_c(\pm kl, y) \\ \overset{\circ}{v}_c(\pm kl, y) \\ \overset{\circ}{w}_c(\pm kl, y) \end{pmatrix} = \begin{pmatrix} (-1)^{mk} h(y) \\ 0 \\ 0 \end{pmatrix}. \tag{4.5}$$

This shows that the solutions (4.4) satisfy the condition $w = 0$ at the rib stations.

With proposition (4.4), the solution of Eq. (4.1) (or equivalently Eqs. (3.18a) and (3.18b)) is reduced to the determination of the transverse profile of the buckling mode $\{h(y), g(y), f(y)\}^T$. The way this will be carried out is described in Section 5.

4.2. General shape of the modification terms

We now consider the general form of the solution for $\overset{\circ\circ}{\mathbf{u}}_c$. It can be verified by inspection, that substitution of the shape functions (4.4) in the first part of Eq. (4.2) yields

$$\mathbf{D}_1^0(\overset{\circ\circ}{\mathbf{u}}) - \lambda_c \mathbf{D}_1'(\overset{\circ\circ}{\mathbf{u}}) = \begin{Bmatrix} H_2(y)\sin 2px \\ G_0(y) + G_2(y)\cos 2px \\ F_0(y) + F_2(y)\cos 2px \end{Bmatrix}. \tag{4.6}$$

The functions of the right-hand side of Eq. (4.6) are thus completely determined by the solution of Eq. (4.1) represented by Eq. (4.4). It can now be shown, by inspection, that the *particular solutions* of the second-order perturbation Eq. (4.2) must be of the form:

$$\overset{\circ\circ}{\mathbf{u}}_c = \begin{Bmatrix} q_0 x + h_2(y)\sin 2px \\ g_0(y) + g_2(y)\cos 2px \\ f_0(y) + f_2(y)\cos 2px \end{Bmatrix}, \tag{4.7}$$

where the scalar q_0 and the functions $h_2(y), g_2(y), f_2(y), g_0(y), f_0(y)$ are still to be determined. The term $(q_0 x)$ for the tangential component (u), which is part of the homogeneous solution of Eq. (4.6) is added here in order to be able to fulfill the requirement that the solution for the modification term $\overset{\circ\circ}{\mathbf{u}}_c$ should not change the total axial load of the panel. The discussion of this particular detail of the construction of $\overset{\circ\circ}{\mathbf{u}}_c$ is postponed to Section 5.3.

The particular solution of Eq. (4.6) satisfies the equilibrium equations with respect to the axial coordinate x, and when the transverse profiles are determined correctly, they also satisfy these equations in the y direction. What can be said about the support conditions at $x = \pm kl$? Rearrangement of Eq. (4.7) gives

$$\overset{\circ\circ}{\mathbf{u}}_c = \begin{Bmatrix} q_0 x + h_2(y)\sin 2px \\ g_0^*(y) + g_2(y)(\cos 2px - 1) \\ f_0^*(y) + f_2(y)(\cos 2px - 1) \end{Bmatrix} \tag{4.8}$$

with $g_0^*(y) = g_0(y) + g_2(y)$, $f_0^*(y) = f_0(y) + f_2(y)$. At the rib stations, these functions thus take the values:

$$\overset{\circ\circ}{\mathbf{u}}_c = \begin{pmatrix} \overset{\circ\circ}{u}_c(\pm kl, y) \\ \overset{\circ\circ}{v}_c(\pm kl, y) \\ \overset{\circ\circ}{w}_c(\pm kl, y) \end{pmatrix} = \begin{pmatrix} \pm kl q_0 \\ g_0^*(y) \\ f_0^*(y) \end{pmatrix}. \tag{4.9}$$

Eq. (4.9) shows that the rib support condition $w = 0$ is not satisfied in general. It can be argued however, that the boundary layer solution that is necessary to complete Eq. (4.8) is insignificant and can be neglected.

It is well known from the non-linear plate theory that the solution of the second-order perturbation equations concerns the redistribution of stresses in the plane of the plate at the instant, the normal buckling displacements $w(x,y)$ start to grow. On the kinematical level, solution (4.8) represents an in-plane displacement field that is compatible with the normal displacement w as soon as this component becomes finite. Thus, while the first-order solution is primarily an out-of plane displacement, the second-order field consists primarily of in-plane components. For example, for a simply supported plate, non-zero components u, v are not present in $\overset{\circ}{\mathbf{u}}_c = \mathbf{a}_c$, i.e., $h = g = 0$ in Eq. (4.4), whereas in $\overset{\circ\circ}{\mathbf{u}}_c = \mathbf{v}$ the situation is reversed i.e., $f_0, f_2 = 0$ in Eq. (4.7). This observation leads to the conclusion that coupling between the in-plane and out-of-plane components – in either of the two fields $\mathbf{a}_c$ and $\mathbf{v}$ – occurs only when the various plate units of the panel meet each other at angles.

It thus follows that coupling between the in-plane components (u,v) and the normal component w in either of the modes $\mathbf{a}_c$ and $\mathbf{v}$ occurs generally, but only in a weak sense. This implies that we expect the contributions of the component w to remain small in the second-order solution $\mathbf{v}$ because it is connected to small contributions of u,v in the buckling mode $\mathbf{a}_c$. According to this reasoning, a rectification of the defect at the rib supports produced by Eq. (4.8) would then correspond only to a negligible change of the total energy of the panel. In other words, the neglect of the support condition $\overset{\circ\circ}{w}_c(\pm kl, y) = 0$ should not have an appreciable influence on the final solution. We conclude these observations by nothing that it is always possible to check the error of our approximation using Eq. (4.9).

5. The finite strip method

5.1. Basic idea

Koiter derived Eqs. (3.17a) and (3.17b) on the basis of two minimum problems (Koiter, 1945). The first reads:

(i) Find the smallest positive value of $\lambda = \lambda_c$ that corresponds to a solution of the problem,

$$\lambda = \min\left\{\frac{P_2^0(\mathbf{u})}{P_2'(\mathbf{u})}\right\} \tag{5.1a}$$

for any admissible but non-vanishing $\mathbf{u}$ satisfying

$$P_2'(\mathbf{u}) = 1. \tag{5.1b}$$

The second problem can be cast into the form:

(ii) Find the function $\mathbf{v}$ that satisfies

$$\min\{P_2^0(\mathbf{v}) - \lambda_c P_2'(\mathbf{v}) + 2P_{21}(\mathbf{u}_c^\circ, \mathbf{v}) + \kappa P_{11}'(\mathbf{a}_c, \mathbf{v})\} \tag{5.2}$$

for any admissible $\mathbf{v}$ and κ. (The parameter κ is here a Lagrange multiplier that enforces the orthogonality condition on $\mathbf{a}_c$ and $\mathbf{v}$, in accordance with Eq. (3.24b)).

To obtain the solutions for the two problems defined above, propositions (4.4) and (4.7) are substituted into Eq. (5.1) and (5.2). This process reduces *both* problems from the dimension two to one, whereby the remaining functions to be determined are the functions $\{h(y), g(y), f(y)\}$; $\{h_0(y), g_0(y), f_0(y)\}$ and $\{h_2(y), g_2(y), f_2(y)\}$, the transverse profiles of the modes (4.4) and (4.7). For their solution, we can introduce a one dimensional discretization procedure. This reduction process is known as the *finite strip* method (Cheung, 1976; Vishwanatan and Tamakuni, 1973; Wittrick and Williams, 1974; Plank and Wittrick, 1974; van der Sloot, 1980; Graves-Smith and Shridharan, 1978; Sridharan and Graves-Smith, 1981; Sridharan, 1982, 1988; Shridharan and Ashraf, 1986). The detailed description of the computer implementation of this development is presented in (Arendsen, 1989). Here, we restrict the discussion to a few comments.

It is noted that at the code level the first-order equations present themselves as

(i) *Problem 1:*

$$\begin{aligned}&[\mathbf{K}^0(p) - \lambda\mathbf{K}'(p)]\mathbf{t} = 0,\\ &\quad \mathbf{t}^{\mathrm{T}}\mathbf{K}'(p)\mathbf{t} - 1 = 0\end{aligned} \tag{5.3}$$

with $p = m\pi/l$, and $m = 1, 2, 3, 4, \ldots$ The N dimensional vector $\mathbf{t}$ denotes here the set of active degrees of freedom that determine the transverse profile of the buckling mode $\overset{\circ}{\mathbf{u}}_c$, whereas $\mathbf{K}(p, \lambda) = \mathbf{K}^\circ(p) - \lambda\mathbf{K}'(p)$ can be identified as the stiffness matrix of the panel determined along the basic state.

It should be realized that the finite strip formulation produces a stiffness matrix $\mathbf{K}$, which is dependent on the wave number $p(m)$ that we selected for the displacement field $\overset{\circ}{\mathbf{u}}_c$ at Eq. (4.3). Consequently, the solutions of the eigenvalue problem (5.3) are dependent on m, i.e., for each value of m, it defines a set of solutions

$$\{\mathbf{t}_i(m), \lambda_i(m)\} : \lambda_1(m) \leqslant \lambda_2(m) \leqslant \lambda_3(m) \leqslant \cdots \leqslant \lambda_N(m) \quad m = 1, 2, 3, \ldots. \tag{5.4}$$

The buckling load that we seek thus corresponds to the minimum of all $\lambda_1(m)$ with respect to m.

(ii) *Problem 2:* The second problem is reduced in a similar fashion. In this case, the discretization process produces two sets of inhomogeneous equations that are written as

$$\mathbf{K}(p_0, \lambda_c)\mathbf{q}_0 = \mathbf{r}_0(\mathbf{q}_c, \lambda_c); \quad p_0 = 0, \tag{5.5a}$$

$$\mathbf{K}(p_2, \lambda_c)\mathbf{q}_2 = \mathbf{r}_2(\mathbf{q}_c, \lambda_c); \quad p_2 = 2p. \tag{5.5b}$$

The sets of discrete variables $\mathbf{q}_0$ and $\mathbf{q}_2$ determine the transverse profile of the field (4.7). Notice, that the path derivative $\overset{\circ}{\lambda}_{\mathrm{II}}$ that characterizes the change of stiffness at the point of buckling is determined by integrals (3.27).

5.2. The transverse interpolation functions

The discretization of the transverse functions h, g and f is accomplished by dividing the transverse cross-section of the panel into strips (Fig. 5). The shape functions that we choose for this transverse element are given by

$$\begin{aligned} h(y) &= b\{(1-\zeta)u_1 + \zeta u_2\},\\ g(y) &= b\{(1-\zeta)v_1 + \zeta v_2\},\\ f(y) &= b\{(1-3\zeta^2+2\zeta^3)w_1 + (\zeta - 2\zeta^2 + \zeta^3)\beta_1 + (3\zeta^2 - 2\zeta^3)w_2 + (-\zeta^2+\zeta^3)\beta_2\}. \end{aligned} \tag{5.6}$$

Here $\zeta = y/b$ denotes the local coordinate of the finite strip of width b, while $u_1, \ldots, \beta_2$ define the nodal degrees of freedom. The assembly of the right-hand sides $\mathbf{r}$ and the stiffness matrices $\mathbf{K}$ in Eqs. (5.3), (5.5a) and (5.5b) then follows a standard pattern.

The evaluation and assembly of the stiffness matrices $\mathbf{K}^0$ and $\mathbf{K}'$ is identical in the two successive problems (5.3), (5.5a) and (5.5b) as these matrices are based on the same shape functions (5.6). The derivation and the coding of the routines that compute the right sides of Eq. (5.5a and b), i.e., the vectors $\mathbf{r}_0$ and $\mathbf{r}_2$ is lengthy and very tedious by hand. It turned out that these functions could be generated with the symbolic manipulation program REDUCE (anonymous, 1984). Consequently, a substantial part of the coding was produced by REDUCE. The evaluation of the integrals $P_4(\mathbf{a}_c)$, $P_2^0(\mathbf{v})$ etc. are carried out by numerical integration. For more details refer to Arendsen (1989).

5.3. The buckling stresses as a self equilibrating system

The formulation as given here relies on the decomposition of the total displacement in the displacements of the trivial state $\lambda\mathbf{U}_0$ and the buckling displacements $\mathbf{u}$

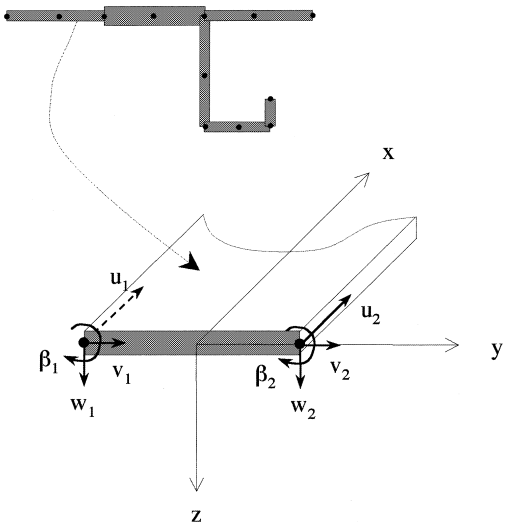

Fig. 5. Finite strip – conventions and notation.

$$\mathbf{U}_{\text{tot}} = \mathbf{U}_{\text{tot}}(\mathbf{x}, \eta) = \lambda \mathbf{U}_0(\mathbf{x}) + \mathbf{u}(\mathbf{x}, \eta), \qquad \lambda = \lambda(\eta), \tag{5.7}$$

with

$$\mathbf{U}_0(\mathbf{x})^{\mathrm{T}} = \{-\varepsilon_0 x, v_0 + v_{12}(\varepsilon_0 y, 0)\}^{\mathrm{T}} \qquad \mathbf{u} = \{u(x,y,\eta), v(x,y,\eta), w(x,y,\eta)\}^{\mathrm{T}}.$$

We recall that the nominal axial strain ε_0 is assumed uniform throughout the panel, whereas the material constant v_{12} may vary with (y). The latter property follows from the fact that different (orthotropic) materials can be used for the construction of the panel cross-section. With the definitions for the buckling displacements made in Section 4, the above expression can be specified as

$$\mathbf{U}_{\text{tot}} = \begin{Bmatrix} -\lambda\varepsilon_0 x \\ v_0 + \lambda v_{12}\varepsilon_0 y \\ 0 \end{Bmatrix} + \left[\eta \begin{Bmatrix} h(y)\cos px \\ g(y)\sin px \\ f(y)\sin px \end{Bmatrix} + \frac{1}{2}\eta^2 \begin{Bmatrix} q_0 x + h_2(y)\sin 2px \\ g_0(y) + g_2(y)\cos 2px \\ f_0(y) + f_2(y)\cos 2px \end{Bmatrix} \right]. \tag{5.8}$$

This displacement field generates an axial stress that we denote by

$$\sigma_{\text{tot}} = \lambda\sigma_0(x,y) + [\Delta\sigma_{\text{m}}(x,y,\eta) + z\ \Delta\sigma_{\text{b}}(x,y,\eta)]. \tag{5.9}$$

Here $\Delta\sigma_{\text{m}}$ is the (averaged) membrane part and $\Delta\sigma_{\text{b}}$ the bending part of the redistribution of stresses due to buckling.

We observe now that the total axial load F_{tot} acting at the ends $(\pm L)$ of the panel must be in equilibrium with the axial stresses $\sigma_{x\text{tot}}$ integrated over the cross-section of the panel at each rib station; thus

$$\begin{aligned} F_{\text{tot}} &= \int_{\text{b}} [\lambda\sigma_{x0} + \Delta\sigma_{\text{m}x}(L,y,\eta)] h_{\text{e}}(y)\,\mathrm{d}y \\ &= \lambda \int_{\text{b}} E_{11}(y)\varepsilon_0 h_{\text{e}}(y)\,\mathrm{d}y + \int_{\text{b}} [\Delta\sigma_{\text{m}x}(l,y,\eta)] h_{\text{e}}(y)\,\mathrm{d}y \\ &= \lambda F_0 + \Delta F_{\text{b}}(\eta). \end{aligned} \tag{5.10}$$

Here, h_{e} denotes the thickness of the plate element.

The above expression shows that, in general case, when no special conditions are imposed on $\mathbf{u}$, we do not end up with λ being proportional to the total load that is acting on the panel. To enforce that λ remains proportional to the total load, we add the term $q_0 x$ (part of the homogeneous solutions of Eq. (4.6)). By adding this term in Eq. (5.8), we can impose the condition

$$\Delta F = \int_{\text{b}} [\Delta\sigma_{\text{m}x}(l,y,\eta)] h_{\text{e}}(y)\,\mathrm{d}y = 0. \tag{5.11}$$

The redistribution of stresses $\Delta\sigma$ connected with the buckling displacements $\mathbf{u}$ is, here, thus constructed in such a way that it forms a self equilibrating system (in axial direction). With this convention, the total load F_{tot} is computed using the expression:

$$F_{\text{tot}} = \lambda \int_{\text{b}} E_{11}(y)\varepsilon_0 h_{\text{e}}(y)\,\mathrm{d}y. \tag{5.12}$$

5.4. The load vs. end-shortening relation

The in-plane component (u) in the x-direction is given by

$$u(x,y) = -\lambda\varepsilon_0 x + \eta h(y)\cos px + \tfrac{1}{2}\eta^2\{q_0 x + h_2(y)\sin 2px\}, \qquad p = k\pi/l \quad k = \text{integer}, \tag{5.13}$$

where the nominal strain ε_0 is defined as positive number. The average shortening e of the panel (defined as a positive number for compression) is then obtained as

$$-e = \frac{1}{b}\int_{\mathrm{b}} \frac{u(l,\psi) - u(-l,\psi)}{2l}\,\mathrm{d}\psi = -\lambda\varepsilon_0 + \frac{1}{2}\eta^2 q_0. \tag{5.14}$$

The combination of Eqs. (3.31) and (5.14) allows us to derive the relations between λ and e:

$$\text{for } \lambda < \lambda_{\mathrm{c}}, \quad \lambda = \frac{e}{\varepsilon_0},$$

$$\text{for } \lambda > \lambda_{\mathrm{c}}, \quad \lambda = \lambda_{\mathrm{c}} + \frac{(e - \lambda_{\mathrm{c}}\varepsilon_0)\overset{\circ\circ}{\lambda}_{\mathrm{cII}}}{\overset{\circ\circ}{\lambda}_{\mathrm{cII}}\varepsilon_0 - q_0}. \tag{5.15}$$

The stiffness of the panel before and after buckling is then characterized by

$$\begin{aligned} &\text{for } \lambda < \lambda_{\mathrm{c}}, \quad \frac{\mathrm{d}\lambda}{\mathrm{d}e} = \frac{1}{\varepsilon_0}, \\ &\text{for } \lambda > \lambda_{\mathrm{c}}, \quad \frac{\mathrm{d}\lambda}{\mathrm{d}e} = \frac{\overset{\circ\circ}{\lambda}_{\mathrm{cII}}}{\overset{\circ\circ}{\lambda}_{\mathrm{cII}}\varepsilon_0 - q_0}. \end{aligned} \tag{5.16}$$

6. Examples and conclusion

6.1. Validation of the code

The validation of the PANBUCK program was carried out with the help of a number of classical problems solved in the literature. We first checked the code using well known examples for which analytical solutions are available. Among these, we mention the results obtained by Koiter and van der Neut in connection with their analysis of a hat-stiffened panel (Koiter and Pignataro, 1976; van der Neut, 1976). In all these cases, the solutions produced by our code matched the solutions presented in the literature in a perfectly satisfactory manner. We will not review these examples in detail here, but instead, present, where the results of the asymptotic method are directly compared with the results of a non-linear finite element analysis.

6.2. The example of a hat-stiffener section

Consider the hat-stiffener–skin section pictured in Fig. 6. We assume that the coupling of the two shell sections is perfect so that the composite parts behave as one shell section with thickness equal to the sum of the two parts. The hat and skin material is homogeneous and isotropic, with the parameter values given in the figure. The section is cut from a wide panel with a large number of stiffeners ($n_{\mathrm{st}} = 10$). The distance between the ribs is $l = 390$ mm.

For the boundary conditions along the longitudinal edges, we choose: $v = 0,\ \beta_x = 0$ at one edge and $v(x) = \text{constant},\ \beta_x = 0$ at the other. With this combination, the hat section may be seen to represent the wide panel as a whole (for local buckling). The eccentricity between the mid surfaces of the single layer parts of the cross-section and the mid surface of composite skin-hat parts will be ignored in this analysis. This means that the shell section is modeled in the way it is pictured in the upper part of Fig. 5.

The details given above complete the description of the finite-strip model. For the finite-element model, (Figs. 8a,b), we introduce a basic configuration that can be used to check the influence of the support conditions at $x = 0$ as we will proceed to show. We take the stiffener-skin section with length l and apply along the longitudinal skin edges of the same boundary conditions that are used for the finite strip model.

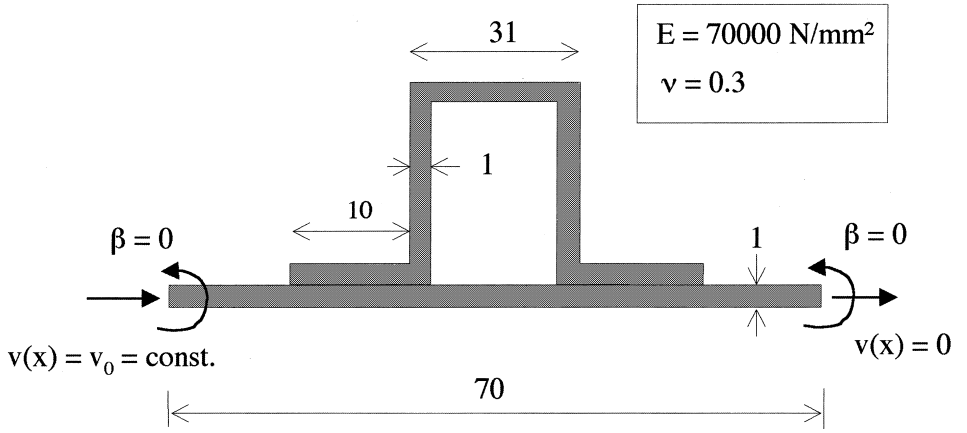

Fig. 6. Hat section layout.

For the two *transverse* edges of this model, i.e., the edges cut by the planes S_-: $x = -(1/2)l$ and S_+: $x = +(1/2)l$, we enforce the conditions: $\beta_y = \beta_z = 0$, together with the stipulation that the axial displacements at these locations are given by $u(-(1/2)l, y) = \Delta l/2$, $u((\frac{1}{2})l, y) = -\Delta l/2$, where Δl is the end-shortening of the model when it is under load. These edge conditions enforce the symmetry of the solutions with respect to the "moving" planes S_-^*: $x = -(1/2)(l - \Delta l)$ and S_+^*: $x = +(1/2)(l - \Delta l)$, respectively. For the suppression of the rigid body mode, we will consider two options. The first corresponds to the elimination of the motion of an arbitrary node in vertical direction. This option renders the STAGS model equivalent to the finite strip model in terms of the possibility to represent modes of the type (5.8). However, as an alternative, it is also possible to replace the last condition by a condition that mimics the support of the ribs in the way we discussed in Section 4. This corresponds to the suppression of the normal displacement w of the skin outside the hat-stiffener area, see Fig. 8b, at the station $x = 0$. The latter variant restricts a proper comparison between both models to cases, where the critical buckling mode exhibits an uneven number of half waves measured over the length of the panel bay. However, this model will still allow us to verify the conjectures that we made regarding the importance of the support conditions as an influence on the post-buckling solutions.

6.2.1. Finite strip analysis

The analysis of the finite-strip model was carried out as follows. We first determined the spectrum of buckling loads and corresponding modes in the range: $p_m = m\pi/l$, $m = 1$–20. This spectrum, see also Fig. 7, reveals that the critical buckling load is given by $P_1 = P_{cr} = 4.454 \times 10^4$ N with a mode with 12 half waves. The second bifurcation load is given by $P_2 = 4.485 \times 10^4$ N with 11 half waves, the next load is $P_3 = 4.485 \times 10^4$ N and has 13 waves, $P_4 = 4.558 \times 10^4$ N with 14 half waves, etc. Global buckling with $p = \pi/l$ of this model takes place at $P_{glob} = 19.144 \times 10^4$ N.

The post-buckling analysis was carried out using the critical mode 1. We note at this point that the single mode post-buckling analyses can only have a limited range of validity because the first six or seven bifurcation points for this panel are very closely spaced. In fact, closely spaced bifurcation points are a forewarning of the possibility of mode jumping phenomena to occur when the load is growing in excess of the buckling load P_1, (Riks et al., 1997). This means, among others that the initial post buckling solution is only stable for $P_1 < P < P_1 + \Delta P$, where ΔP is small in comparison of P_1 (in this particular case it turns out that $\Delta P \approx 0.3\ P_1$). For the verification of our code, this issue is not directly relevant, but we mention it nevertheless to warn potential users for the possible pitfalls in the evaluation of its results.

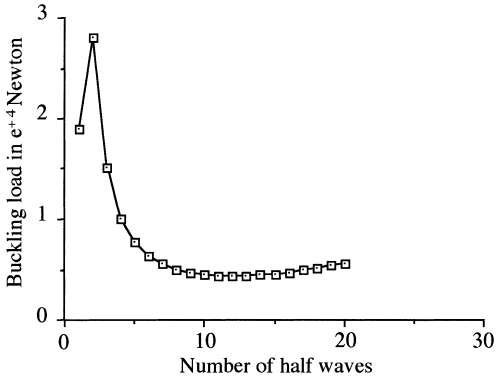

Fig. 7. Buckling load spectrum.

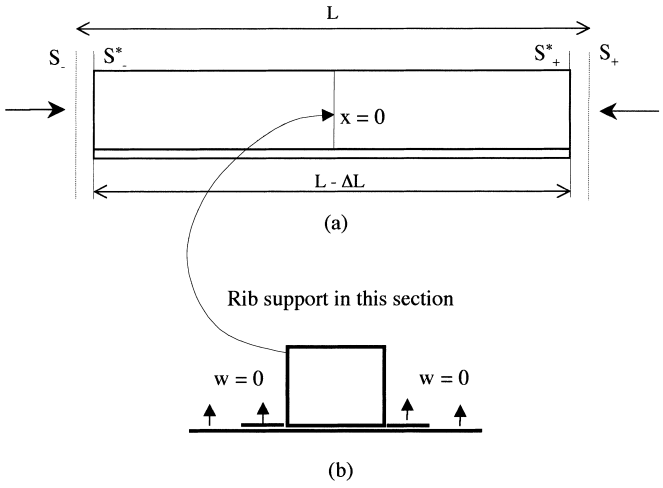

Fig. 8. Some details of the STAGS model.

6.2.2. Finite element analysis

The finite element model that we described earlier was constructed using the STAGS code (Rankin et al., 1998). With this model (and its variants), we carried out the following analyses. First, we determined the critical-buckling load and corresponding mode of the model for the case $l = 390$ mm. After that, we computed the bifurcation diagram using the path, following methods that are available in the STAGS program.

This analysis produced the following results: (i) the critical-buckling load and the corresponding mode, (ii) the reduction of stiffness after buckling at the first bifurcation point. We were also able to determine the secondary bifurcation point along the first post-buckling state II, after which this state II becomes unstable so that a mode jump will take place (Table 1).

Fig. 9 presents an image of the critical buckling mode for the model in the absence of support conditions at $x = 0$, which also shows the mesh that was used. Fig. 10 gives STAGS results in terms of the "load vs. end-shortening" and "load vs. normal displacement" plots for this case. The key results of this and the previous

Table 1
Hat-stiffener, first result

	STAGS	PANBUCK
P_{cr} (N)	0.4474 10^{+5}	0.4454 10^{+5}
λ_{cr}	1.0045	1
Number of half waves	12	12
$\frac{d\Lambda}{dE}\Big\|_{II} = \frac{e_{cr}}{\lambda_{cr}} \frac{d\lambda}{de}\Big\|_{II}$	0.707	0.708

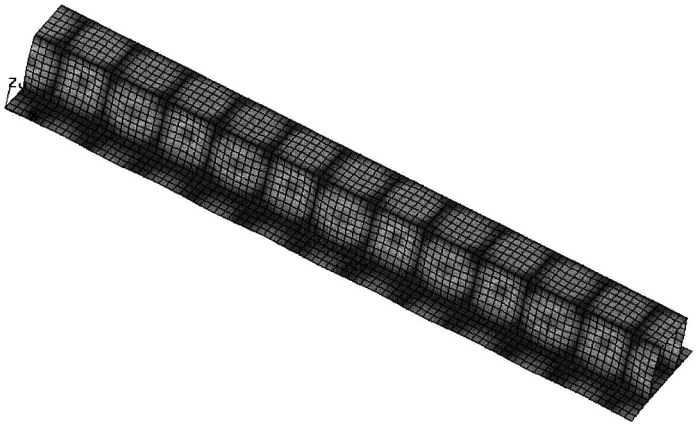

Fig. 9. The critical buckling mode (support conditions at $x = 0$ not enforced).

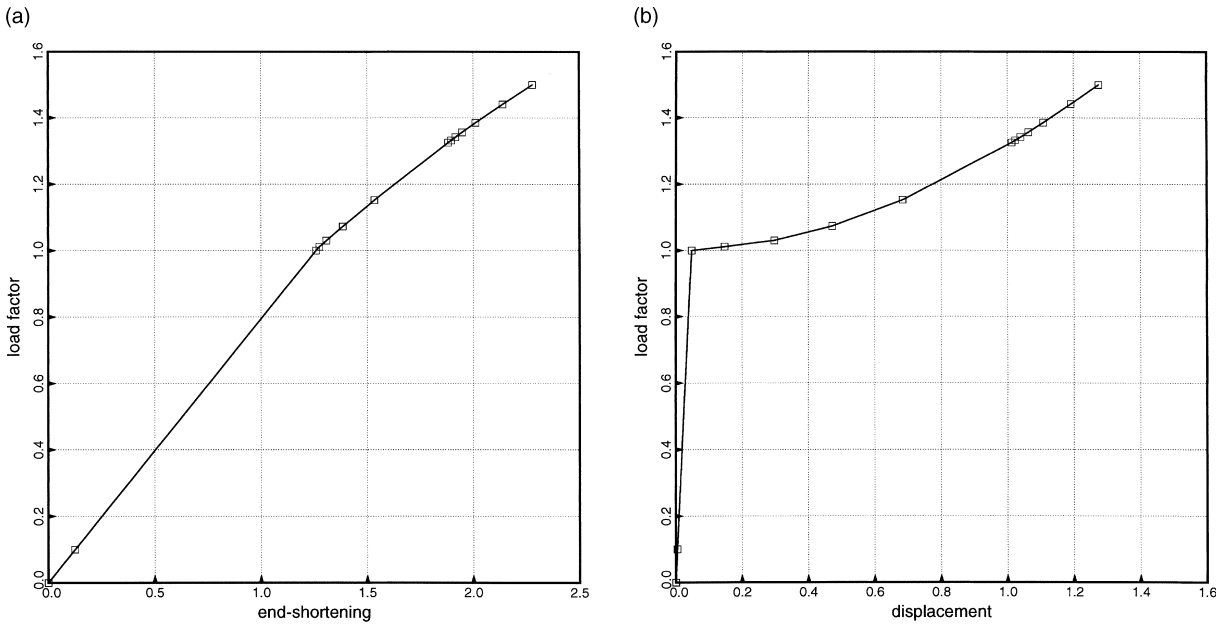

Fig. 10. Panel response according to STAGS. (a) Load vs. end-shortening. (b) Load vs. normal displacement.

finite strip analysis are given in Table 1. We note here that the STAGS result for the drop in stiffness after buckling was determined using the finite difference expression:

$$\left.\frac{\mathrm{d}\Lambda}{\mathrm{d}E}\right|_{\mathrm{II}} = \frac{\Delta l_{\mathrm{cr}}}{\lambda_{\mathrm{cr}}}\left.\frac{\mathrm{d}\lambda}{\mathrm{d}\Delta l}\right|_{\mathrm{II}} \approx \frac{\Delta l_{\mathrm{cr}}}{\lambda_{\mathrm{cr}}}\frac{\lambda_1-\lambda_{\mathrm{cr}}}{\Delta l_1-\Delta l_{\mathrm{cr}}} \tag{6.1}$$

in which Δl denotes the end-shortening of the model, λ denotes the load-factor (normalized with respect to the critical value produced by PANBUCK), and where the subscript 1 refers to the values that correspond to the first solution beyond the critical point $(\lambda_{\mathrm{cr}}, \Delta l_{\mathrm{cr}})$.

6.2.3. The influence of the support conditions

To evaluate the influence of the support conditions on the behavior of the model, we also conducted a buckling and post-buckling analysis with the STAGS model, in the case that the support conditions defined in Fig. 8b, are active. We already mentioned that with this modification, the STAGS model can no longer admit buckling modes that are harmonic in the axial direction, see Eqs. (4.4) and (5.8) with an even number of half waves m between the rib stations. The reason is that these modes, in terms of the components v and w, cannot satisfy the symmetry conditions at the moving planes S^*_- and S^*_+ and the simple support conditions $x = 0$ at the same time. Only (harmonic) modes with an uneven number of half waves m can satisfy these requirements.

However, the STAGS model can produce other types of modes, which exhibit an even number of half waves, but which are no longer harmonic. This is what occurred in the present analysis. The critical buckling mode in this case still has 12 half waves although there is now a slight modification in shape of this mode in comparison with the mode of the previous STAGS case. The modification occurs in the region of the support at $x = 0$. We will not present the branching diagrams and the pictures of the modes for this case because they are hardly different from the previous ones. We only present here, in Table 2, the cardinal results concerning the buckling load and post-buckling stiffness computed by STAGS (the PANBUCK results remain unaltered but are included for convenience).

It is thus observed that the support conditions that mimic the presence of the rib stations have hardly any effect on the outcome of the STAGS analysis. This confirms our conjecture regarding the effect of the rib supports. It also illustrates how effective finite strip solutions are for this case.

6.2.4. Discussion

Of course, the post-buckling solution produced by PANBUCK is only a first approximation. In the load vs. end-shortening plot this approximate solution corresponds to a straight line. The STAGS solution (Fig. 10a) shows how the "actual" post-buckling path deviates from the straight line. We can infer from the difference between these two solutions how accurate the asymptotic method is in this case.

In agreement with our expectations described in Eq. (4.2). the STAGS analysis confirms that the neglect of the support conditions in the construction of the post-buckling terms is justified, at least in this particular case of local buckling. Tentative investigations, which we will not further discuss here, have shown that also in the case of global modes, $n = 1$, the post-buckling solution produced by PANBUCK remains reliable.

Table 2
Hat-stiffener, second result

	STAGS	PANBUCK
P_{cr} (N)	$0.4485\ 10^{+4}$	$0.4454\ 10^{+4}$
λ_{cr}	1.0078	1
Number of half waves	12	12
$\left.\frac{\mathrm{d}\Lambda}{\mathrm{d}E}\right\|_{\mathrm{II}} = \frac{e_{\mathrm{cr}}}{\lambda_{\mathrm{cr}}}\left.\frac{\mathrm{d}\lambda}{\mathrm{d}e}\right\|_{\mathrm{II}}$	0.708	0.708

Lack of space prevents us to go into a discussion of these cases here. We will return to them at another place.

The post-buckling branch II, as computed by STAGS (Fig. 10) becomes unstable at a point determined by $\lambda = 1.324$. At this bifurcation point, the panel will suffer a mode jump. The jump most probably ends at a stable branch characterized by a mode with 14 half waves. A snap of this nature is rather mild and does not result in the destruction of the panel. After further loading, this secondary stable post-buckling path will become unstable again and another mode jump will occur, (we guess to a state with 16 half waves), and so on. We did not investigate this response sequence here, because it takes considerable effort to analyze, but we are rather confident that this is the global behavior we can expect (Riks et al., 1997). This observation implies that the usefulness of the present PANBUCK solution for $n = 12$ is limited to the load value of $\lambda = 1.324$. To what extent the finite strip solutions for the modes $n = 14$, $n = 15$, etc. can be used to represent the states, the structure jumps to for values of $\lambda > 1.324$ is a question that needs further investigation.

6.3. An example of a Z-stiffened panel

We will conclude the discussion by showing another aspect of the possibilities that are offered by this application of Koiter's post-bifurcation theory. In this case, we selected a panel that is 800 mm long and 13×80 mm wide. It has a curvature of $R = 3000$ mm and is equipped with 13 Z-stiffeners. The geometry of the stiffener is given in Fig. 11. Along the longitudinal edges of the panel only the displacements in the global z-direction are suppressed. Although the finite strips by themselves are flat prismatic elements, the cylindrical parts of the panel can still be modeled by these strips in the same way that the flat STAGS quadrilateral elements are capable to model doubly curved shells.

The buckling analysis by PANBUCK reveals that the critical buckling mode of this panel has 12 half waves in axial direction. This (local) mode is pictured in Fig. 12 covering one half of the panel length l. The post-buckling analysis computes the post-buckling stiffness at $\left(\frac{d\Lambda}{dE}\right)\Big|_{II} = 0.73$.

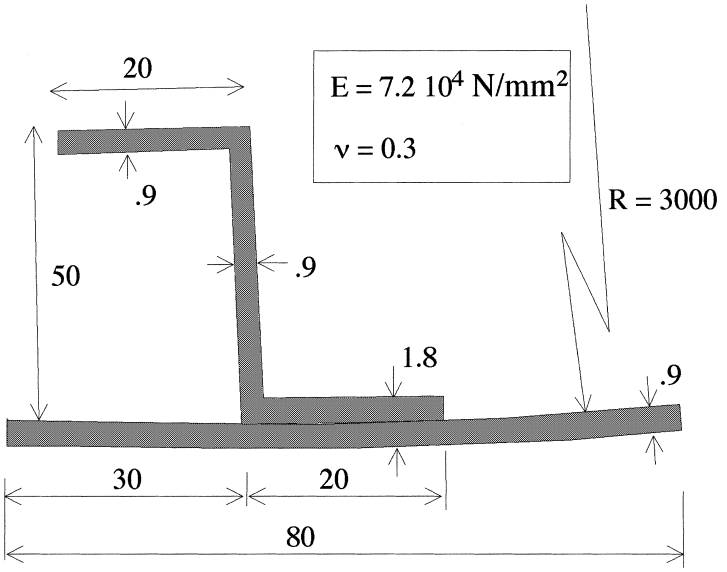

Fig. 11. Z-stiffened panel, dimensions in mm.

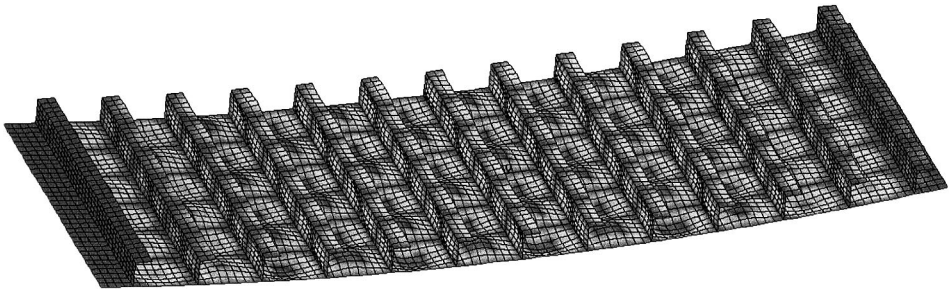

Fig. 12. Initial post-buckling state of the panel.

The example given here corresponds to a case, where it is not admissible to derive the basic characteristics of the buckling and post-buckling behavior of the panel by simply reducing the problem to an isolated stiffener section. This is a conclusion that generally holds good for panels that do not have a high degree of regularity in the layout of the cross-section. For such type of problems, the finite strip formulation discussed here holds an advantage in comparison with methods that are based on averaging principles.

6.4. Conclusion and recommendations

(i) The finite strip method is a fast method. The volume of the computations is relatively modest as compared to the volume of computations that are connected with two-dimensional shell finite element analyses. These characteristics explain why this method is useful in the preliminary design of wing box panels (Stroud and Anderson, 1980) and why the present method is incorporated in the optimization code for preliminary design PANOPT (Arendsen and Wiggenraad, 1991; Arendsen, 1993).

(ii) The model that is developed here is expected to give accurate results within the scope of the assumptions made. If not all assumptions are met, the results of the post-buckling analysis must be interpreted with care (see also the discussion in Section 4.2). The range of validity in terms of $\Delta\lambda = \lambda - \lambda_c > 0$ is expected to be somewhat in the neighborhood of $\Delta\lambda < 0.5\lambda_c$ in the case of simple bifurcation, but it can never be established before-hand as it depends on the problem at hand. It is always a good idea to cross check the results, either by comparing them to classical solutions (when available) or by cross-checking it with a finite element analysis. This is in any case a good practice, no matter what design process is used.

(iii) In this article, we avoided the question of how to deal with bifurcation points that are very close together. This question can be important in the case that global buckling takes place together with some local modes (Budiansky, 1974; Shridharan, 1983; Shridharan and Ashraf, 1986; Koiter and Pignataro, 1976; van der Neut, 1976). In PANBUCK, provisions for the multi-mode case have already been made (the construction of the $\mathbf{v}_{ij}$ terms in that case) but more work is required to make this particular case operational (Riks, 1989; Arendsen, 1989).

(iv) Koiter and Pignataro (1976) developed closed form solutions for the interaction of local and global-buckling modes, which are defined by integrals that involve the buckling modes and modification terms. As these terms are produced by our code, i.e. the terms $\mathbf{a}_c$ and $\mathbf{v}$, this "amplitude modulation" approach can easily be incorporated.

(v) The perturbation solutions that are presented here are developed at the bifurcation point determined by λ_c. Improvement of the validity of the expansion can be obtained if the perturbation is carried out at points of the fundamental state I that vary with the value of the load λ, e.g. (Koiter, 1945, 1976). It is comparatively easy to change the formulation of the present coding to account for this modification. The

second order term $\mathbf{v}$ is then dependent on the load intensity λ and the calculation must then be carried out pointwise, i.e., for a number of values of λ.

(vi) There may be a need to include imperfections of the initial panel shape into the formulation, in particular in the multi-mode case. The way this can be done is discussed in Appendix B.

Acknowledgements

The author expresses his appreciation for many valuable observations of the reviewers, which led to many improvements. He wants to thank his ex-colleagues at the National Aerospace Laboratory, Paul Arendsen, André de Boer, and Jaap Wiggenraad for their encouragement and support. The able help of Joris Remmers, Delft University of Technology for the preparation of the example problems is also gratefully acknowledged.

Appendix A. Notation

The notation employed in Section 2 and 3 was introduced by Koiter (1945), see also Koiter (1976). As can be deduced from definitions (2.3) and (3.1), the potential energy $P(\mathbf{u})$ is a surface integral, the integrand of which is a sum of products of the arguments, i.e., the derivatives: $u', v', w', \mathring{u}, \mathring{v}, \mathring{w}, w'', w'^{\circ}, \mathring{\mathring{w}}$. (We use here the notation: $(\,)' = \partial/\partial x$, $(\,)^{\circ} = \partial/\partial y$, etc.). The lowest degree of these products in $P(\mathbf{u})$ is two, the highest degree is 4. If we denote the arguments by $z_i (i = 1, 2, 3, \ldots, 9)$ so that $z_1 = u'$, $z_2 = v'$, etc., the terms P_2, P_3, P_4 in expansion (3.2) can be written in the form:

$$P_2(\mathbf{u}) = P^0(\mathbf{u}) - \lambda P'(\mathbf{u}) = \int\int [\Sigma C_2^{0ij} z_i z_j]\,\mathrm{d}S - \lambda \int\int [\Sigma C_2'^{ij} z_i z_j]\,\mathrm{d}S,$$

$$P_3(\mathbf{u}) = \int\int [\Sigma C_3^{ijh} z_i z_j z_h]\,\mathrm{d}S, \tag{A.1}$$

$$P_4(\mathbf{u}) = \int\int [\Sigma C_4^{ijhk} z_i z_j z_h z_k]\,\mathrm{d}S.$$

The coefficients $C_2^{0ij}, C'2^{ij}, C_3^{ijk}, C_4^{ijkh} (i, j, h, k) = 1, 2 \ldots, 9$ are constants. These polynomial forms have the following properties:

If $\mathbf{u} = \mu\mathbf{v}$, where μ is a scalar,

$$P_2(\mu\mathbf{v}) = \mu^2 P_2(\mathbf{v}), \quad P_3(\mu\mathbf{v}) = \mu^3 P_3(\mathbf{v}), \quad P_4(\mu\mathbf{v}) = \mu^4 P_4(\mathbf{v}). \tag{A.2}$$

If $\mathbf{u}$ is given by the sum $\mathbf{u} = \mathbf{v} + \mathbf{w}$, we can write

$$\begin{aligned} P_2(\mathbf{v}+\mathbf{w}) &= P_2(\mathbf{v}) + P_{11}(\mathbf{v},\mathbf{w}) + P_2(\mathbf{w}), \\ P_3(\mathbf{v}+\mathbf{w}) &= P_3(\mathbf{v}) + P_{21}(\mathbf{v},\mathbf{w}) + P_{12}(\mathbf{v},\mathbf{w}) + P_3(\mathbf{w}), \\ P_4(\mathbf{v}+\mathbf{w}) &= P_4(\mathbf{v}) + P_{31}(\mathbf{v},\mathbf{w}) + P_{22}(\mathbf{v},\mathbf{w}) + P_{13}(\mathbf{v},\mathbf{w}) + P_4(\mathbf{w}), \end{aligned} \tag{A.3}$$

which are expansions that are similar to the binomial expansion of the product $(a+b)^n$, $n = 2$–4.

For example, the forms $P_{31}(\mathbf{v},\mathbf{w})$, $P_{21}(\mathbf{v},\mathbf{w})$, etc. are given by

$$P_{31}(\mathbf{v},\mathbf{w}) = 4\int\int [\Sigma C_4^{ijhk} z_i^1 z_j^1 z_h^1 z_k^2]\,\mathrm{d}S, \quad P_{21}(\mathbf{v},\mathbf{w}) = 3\int\int [\Sigma C_3^{ijh} z_i^1 z_j^1 z_h^2]\,\mathrm{d}S, \text{ etc.}, \tag{A.4}$$

where $\mathbf{v} = [z_1^1, z_2^1, \ldots, z_9^1]$ and $\mathbf{w} = [z_1^2, z_2^2, \ldots, z_9^2]$. The factors 4, 3, etc. follow from the binomial coefficient, $\binom{n}{n-m} = \frac{4!}{3!1!} = 4$, $\frac{3!}{2!1!} = 3$, etc. Please note that

$$P_{31}(\mathbf{v},\mathbf{w}) = P_{13}(\mathbf{w},\mathbf{v}), \qquad P_{21}(\mathbf{v},\mathbf{w}) = P_{12}(\mathbf{w},\mathbf{v}), \quad \text{etc.} \tag{A.5}$$

If $\mathbf{v} = \mathbf{w}$ in Eq. (A.4)

$$P_{31}(\mathbf{v},\mathbf{v}) = \binom{4}{4-1} P_4(\mathbf{v}) = 4P_4(\mathbf{v}), \quad P_{21}(\mathbf{v},\mathbf{v}) = \binom{3}{3-1} P_3(\mathbf{v}) = 3P_3(\mathbf{v}), \quad \text{etc.} \tag{A.6}$$

Also, if, in Eq. (A.4), $\mathbf{v} = \mathbf{a} + \mathbf{b}$, then follows:

$$P_{31}(\mathbf{a}+\mathbf{b},\mathbf{w}) = P_{31}(\mathbf{a},\mathbf{w}) + P_{211}(\mathbf{a},\mathbf{b},\mathbf{w}) + P_{121}(\mathbf{a},\mathbf{b},\mathbf{w}) + P_{31}(\mathbf{b},\mathbf{w}). \tag{A.7}$$

If in Eq. (A.7) $\mathbf{a} = \mathbf{b} = \mathbf{w}$, then

$$P_{211}(\mathbf{a},\mathbf{a},\mathbf{a}) = 2P_{22}(\mathbf{a},\mathbf{a}) = 2\binom{4}{4-2} P_4(\mathbf{A}) = 12P_4(\mathbf{a})$$

and so on.

Appendix B. Imperfections

The governing equations are generated by the energy functional:

$$P(\mathbf{u},\lambda) = -\lambda \int_S \mathbf{N}^{\mathrm{T}} \mathbf{l}_2(\mathbf{u})\, \mathrm{d}S + \frac{1}{2}\int_S \boldsymbol{\gamma}^{\mathrm{T}} \mathbf{C}\boldsymbol{\gamma}\, \mathrm{d}S + \frac{1}{2}\int_S \boldsymbol{\kappa}^{\mathrm{T}} \mathbf{B}\boldsymbol{\kappa}\, \mathrm{d}S. \tag{B.1}$$

The following listing explains the significance of the symbols used:

$\mathbf{u}$	the displacement in the buckled state measured with respect to the basic state I
λ	the load factor
$\mathbf{N}_0^{\mathrm{T}}$	the pre-buckling stress field (nominal values)
$\mathbf{I}_2(\mathbf{u})$	quadratic part of the membrane strain measures used
$\boldsymbol{\gamma}$	the mid-surface, Green Lagrange strains
$\boldsymbol{\kappa}$	the changes of curvature
$\mathbf{C}, \mathbf{B}$	the membrane and bending stiffness matrix, respectively
S	the area of integration

This expression was derived with respect to the geometry of the basic state $\mathbf{I} = (-\lambda \mathbf{U}_0)$ but it can with a good approximation, also be regarded to be derived with respect to the geometry of the undeformed state. We will depart from the last supposition, because that point of view will simplify the discussion.

When there are imperfections, the undeformed state is given by $\mathbf{0} + \mu\mathbf{w}_0$. If the structure undergoes a displacement $\mathbf{u}$ under a load $\lambda\mathbf{F}$, the strain measures for the new state $(0 + \mu\mathbf{w}_0 + \mathbf{u})$ are given by the difference between the metric tensors of state $(0 + \mu\mathbf{w}_0 + \mathbf{u})$ and $(0 + \mu\mathbf{w}_0)$, thus,

$$\gamma_{ij}^{*} = \tfrac{1}{2}\{g_{ij} - g_{ij}^{0}\} \tag{B.2a}$$

or in vector form:

$$\boldsymbol{\gamma}^{*} = \tfrac{1}{2}\{\mathbf{g} - \mathbf{g}^{0}\} \tag{B.2b}$$

where superscript $(^0)$ refers to the undeformed state: $(0 + \mu\mathbf{w}_0)$. It can be verified (by inspection) that this leads to

$$\boldsymbol{\gamma}^{*} = \boldsymbol{\gamma}(\mu\mathbf{w}_0 + \mathbf{u}) - \boldsymbol{\gamma}(\mu\mathbf{w}_0) = \boldsymbol{\gamma}(\mathbf{u}) + \mathbf{l}_{11}(\mu\mathbf{w}_0, \mathbf{u}), \tag{B.3}$$

where $\boldsymbol{\gamma}$ corresponds to the Green–Lagrange strain measures and $\boldsymbol{\gamma}$ is given by $\boldsymbol{\gamma} = \mathbf{l}_1(\mathbf{u}) + \mathbf{l}_2(\mathbf{u})$, see Eq. (2.13). The operators $\mathbf{l}_1$ and $\mathbf{l}_2$ are defined by Eq. (2.3 and 2.4), and $\mathbf{l}_{11}(\mathbf{u},\mathbf{v})$ is the bilinear form that is

derived from $\mathbf{l}_2$. It is noted that the curvature changes $\boldsymbol{\kappa}$ are linear operators and therefore not affected by the geometry change.

The modification of the energy functional that results, if we account for initial imperfections, follows if we insert $\mu\mathbf{w}_0 + u$ in Eq. (B.1) in place of $\mathbf{u}$, and $\boldsymbol{\gamma}^*$ given by Eq. (B.3) in place of $\boldsymbol{\gamma}$. This leads to

$$P^*(\mathbf{u},\lambda) = P(\mathbf{u},\lambda) + \mu\lambda Q_1(\mathbf{u}) + \mu Q_3(\mathbf{u}) + \mu^2 Q_2(\mathbf{u}) \tag{B.4}$$

with $P(\mathbf{u},\lambda)$ given by Eq. (B.1) and:

$$\begin{aligned} Q_1(\mathbf{u}) &= -\int_S \mathbf{N}_\mathrm{I}^\mathrm{T}\mathbf{l}_{11}(\mathbf{w}_0,\mathbf{u})\,\mathrm{d}S,\\ Q_2(\mathbf{u}) &= \int_S \boldsymbol{\gamma}^\mathrm{T}(\mathbf{u})\mathbf{C}\mathbf{l}_{11}(\mathbf{w}_0,\mathbf{u})\,\mathrm{d}S,\\ Q_3(\mathbf{u}) &= \frac{1}{2}\int_S \mathbf{l}_{11}^\mathrm{T}(\mathbf{w}_0,\mathbf{u})\mathbf{C}\mathbf{l}_{11}(\mathbf{w}_0,\mathbf{u})\,\mathrm{d}S. \end{aligned} \tag{B.5}$$

Usually, the imperfections are studied only for small values of μ. In this case, the most important contribution leading to the modification is given by the first term $\mu\lambda Q_1(\mathbf{u})$. This follows, because the first integral is of the order of magnitude $\mu\lambda\eta|Q_1(\mathbf{u}_\mathrm{c})|$, whereas the remaining two integrals are of the order of magnitude $\mu^2\eta^2|Q_2(\mathbf{u}_c)|$ and $\mu\eta^3|Q_3(\mathbf{u}_\mathrm{c})|$. Thus, for small amplitudes of the buckling displacements and small imperfections i.e., $|\eta| \ll 1$ and $|\mu| \ll 1$, it is reasonable to neglect the remaining two contributions. With the last observation, the energy expression is brought to the form:

$$P^*(\mathbf{u},\lambda) = P(\mathbf{u},\lambda) + \mu\lambda Q_1(\mathbf{u}). \tag{B.6}$$

According to the general theory (Koiter, 1970, 1976), we can now obtain the behavior of the imperfect panel using the data that we obtained for the perfect case, i.e., the solution

$$\mathbf{u} = \mathbf{a}_\mathrm{c}\eta + \tfrac{1}{2}\mathbf{v}\eta^2. \tag{B.7}$$

Substitution of Eq. (B.7) into Eq. (B.6) yields

$$P^*(\eta,\lambda) = P(\mathbf{a}_\mathrm{c}\eta + \tfrac{1}{2}\mathbf{v}\eta^2,\lambda) + \mu\lambda[Q_1(\mathbf{a}_\mathrm{c}\eta) + \underline{\tfrac{1}{2}\eta^2 Q_1(\mathbf{v})}], \tag{B.8}$$

where the underlined term can be neglected. The equilibrium equation that governs the imperfect panel then follows from the requirement,

$$\frac{\partial P^*(\eta,\lambda)}{\partial\eta} = 0.$$

This finally leads to the *imperfect* bifurcation equation, which after neglect of the terms of order η^4 and higher can be written as

$$\mu\lambda Q_1(\mathbf{a}_\mathrm{c}) + 2(\lambda_\mathrm{c} - \lambda)P_2'(\mathbf{a}_\mathrm{c})\eta + 4\{P_4(\mathbf{a}_\mathrm{c}) - \tfrac{1}{4}[P_2^0(\mathbf{v}) - \lambda_\mathrm{c}P_2'(\mathbf{v})]\}\eta^3 + \mathrm{O}(\eta^4) = 0. \tag{B.9}$$

References

Anon., 1984. REDUCE, Users Manual, Hearn, A.C. (Ed.). The Rand Corporation, Santa Monica, CA 90406. Rand Publication CP78 Rev. 4/84.

Arendsen, P., 1989. Post-buckling analysis using the finite strip method: Derivation of the 2nd, 3rd, 4th, order energy terms, NLR TR 89386 L, The National Aerospace Laboratory, NLR, Anthony Fokkerweg, Amsterdam, Netherlands.

Arendsen, P., Wiggenraad, J.F.M., 1991. PANOPT, User's Manual, NLR CR 91255, The National Aerospace Laboratory, NLR, Anthony Fokkerweg, Amsterdam, Netherlands.

Arendsen, P., 1993. PANOPT, Theoretical Manual, CR 93354, The National Aerospace Laboratory, NLR, Anthony Fokkerweg, Amsterdam, Netherlands.

Benthem, J.P., 1959. The Reduction in Stiffness of Combinations of Rectangular Plates in Compression Exceeding the Buckling Load. NLL TR S. 539, National Aerospace Laboratory, NLR, Anthony Fokkerweg, Netherlands.

Budiansky, B., 1974. Theory of buckling and post-buckling behavior of elastic structures. In: Yih, C.S. (Ed.), Advances in Applied Mechanics, vol. 14. Academic Press, New York, pp. 1–65.

Cheung, Y.K., 1976. Finite Strip Method in Structural Analysis. Pergamon Press, New York.

Graves Smith, T.R., Shridharan, S., 1978. A finite strip method for the post-locally-buckled analysis of plate structures. International Journal Mechanical Sciences 20, 833–843.

Koiter, W.T., 1945. On the stability of elastic stability, Ph.D. thesis, H.J. Paris, Amsterdam, (in Dutch). Translation from the Dutch, 1970, On the stability of elastic stability, AFFDL-TR-7025, Airforce Flight Dynamics Laboratory, Dayton Ohio.

Koiter, W.T., 1966. On the Nonlinear Theory of Thin Elastic Shells. Proc. Kon. Acad. Wet., Amsterdam, pp. 1–54.

Koiter, W.T., 1967. General equations of elastic stability for thin Shells. Proceedings Symposium on the Theory of Shells in Honor of Loyd Hamilton Donnell, University of Houston, USA.

Koiter, W.T., 1976. Current trends in the theory of buckling. Proceedings of the IUTAM Symposium on Buckling of Structures. Harvard University. Springer, Berlin, pp. 1–16.

Koiter, W.T., Pignataro M.A., 1976. General Theory of the Interaction of Local and Overall Buckling of Stiffened Panels. WTHD 83. Department of Applied Mechanics, Technical University Delft, Netherlands.

Plank, R.J., Wittrick, W.H., 1974. Buckling under combined loading of thin-flat walled structures by a complex finite strip method. International Journal for Numerical Methods in Engineering 8, 323–339.

Przemieniecki, J.S., 1973. Finite element structural analysis of local instability. AIAAJ 11, 33–39.

Rankin, C.C., Brogan, F.A., Loden, W., Cabiness, H., 1998. Structural Analysis of General Shells, STAGS User manual, version 3.0, LMMS P032594. Advanced Technology Center, Locksheed Martin, Palo Alto, CA.

Riks, E., 1983. Post-buckling analysis of stiffened panels by the finite strip method. Technical Memorandum SC-83-035 L, National Aerospace Laboratory, NLR, Anthony Fokkerweg, Amsterdam, Netherlands.

Riks, E., 1984. Computational aspects of the stability analysis of nonlinear structures. Computer Methods in Applied Mechanics and Engineering 47, 219–259.

Riks, E., 1989. A finite strip method for the buckling and post-buckling analysis of stiffened panels in wing box structures. NLR CR 89383 L, National Aerospace Laboratory, NLR, Anthony Fokkerweg, Amsterdam, Netherlands.

Riks, E., 1997. Buckling of elastic structures: A computational approach, In: Van der Giessen E. (Ed.), Advances in Applied Mechanics, vol. 34, 1997, Academic Press, Cambridge Mass., pp. 1–70.

Shridharan, S., Ashraf A.M, 1986. An improved interactive buckling analysis of thin-walled columns having doubly symmetric sections. International Journal of Solids and Structures 22 (4), 429–443.

Sridharan, S., Graves-Smith, T.R., 1981. Post-buckling analysis with finite strips. Journal of Engineering Division ASCE EM5, 16551.

Sridharan, S., 1982. A semi-analytical method for the post-local torsional buckling analysis of prismatic plate structures. International Journal for Numerical Methods in Engineering 18, 1685–1697.

Shridharan, S., 1983. Doubly symmetric interactive buckling of plate structures. International Journal of Solids and Structures 19 (7), 625–641.

Stroud, J.W., Anderson M.S. PASCO: Structural Panel Sizing, Code-Capability and Analytical Foundations. NASA Techn. Memo 80181, January 1980.

Van der Neut, A., 1952. The Local Instability of Compression Members Built up from Flat Plates. Report No. 47, Department of Aeronautics, Delft University of Technology, Delft, Netherlands.

Van der Neut. A., 1976. Mode interaction with stiffened panels. Proceedings IUTAM Symposium on Buckling of Structures 1974, Harvard University, Springer, Berlin, pp. 117–132.

Van der Sloot, J.H., 1980. Recent advances with the "experimental method Fokker, EMF" to predict critical loads of stringer stiffened panels. ICAS paper 20.1. Proceedings 12th Congress International Council of the Aeronautical Sciences.

Vishwanatan, A.V., Tamakuni, M., 1973. Elastic Buckling: A Program for Composite panels and Other Structures Subjected to Bi-axial in-Plane Loads. NASA, CR2216.

Wittrick, W.H., 1986. A Unified Approach to the Initial Buckling of Stiffened Panels in Compression. Aeronautical Quaterly, vol. XIX.

Wittrick, W.H., Williams F.W, 1974. Buckling and vibration of anisotropic or isotropic plate assemblies under combined loadings. International Journal of Mechanical Sciences 16, 209–239.